

Evolving Language Models without Labels: Majority Drives Selection, Novelty Promotes Variation

Yujun Zhou^{1,2†*}, Zhenwen Liang^{1†}, Haolin Liu^{1,3}, Wenhao Yu¹, Kishan Panaganti¹,
Linfeng Song¹, Dian Yu¹, Xiangliang Zhang², Haitao Mi¹, Dong Yu¹

¹Tencent AI Lab, ²University of Notre Dame, ³University of Virginia

† Core contributors

Correspondence to: yzhou25@nd.edu, zhenwzliang@global.tencent.com

Abstract

Large language models (LLMs) are increasingly trained with reinforcement learning from verifiable rewards (RLVR), yet real-world deployment demands models that can self-improve without labels or external judges. Existing self-improvement approaches primarily rely on self-confirmation signals (e.g., confidence, entropy, or consistency) to generate rewards. This reliance drives models toward over-confident, majority-favored solutions, causing an entropy collapse that degrades pass@ n and reasoning complexity. To address this, we propose EVOL-RL, a label-free framework that mirrors the evolutionary principle of balancing selection with variation. Concretely, EVOL-RL retains the majority-voted answer as an anchor for stability, but adds a novelty-aware reward that scores each sampled solution by how different its reasoning is from other concurrently generated responses. This *majority-for-stability + novelty-for-exploration* rule mirrors the variation–selection principle: *selection prevents drift, while novelty prevents collapse*. Evaluation results show that EVOL-RL consistently outperforms the majority-only baseline; e.g., training on label-free AIME24 lifts Qwen3-4B-Base AIME25 pass@1 from baseline’s 4.6% to 16.4%, and pass@16 from 18.5% to 37.9%. EVOL-RL not only prevents in-domain diversity collapse but also improves out-of-domain generalization (from math reasoning to broader tasks, e.g., MMLU-Pro and BBEH).

 [Code](#)  [Models](#)

1 Introduction

The reasoning capabilities of Large Language Models (LLMs) have advanced dramatically, particularly through paradigms like Reinforcement Learning with Verifiable Rewards (RLVR) (Jaech et al., 2024; Guo et al., 2025; Yang et al., 2025). The next frontier of intelligence lies in enabling LLMs to autonomously evolve, continuously learning from the vast, unlabeled data streams they encounter in real-world environments. This *label-free evolving* paradigm allows a model to iteratively improve itself while solving tasks, without relying on ground-truth labels or external judges, making it both practical and necessary. However, turning inference into learning reopens a long-standing RL problem: balancing exploration and exploitation. This dilemma becomes especially severe in label-free settings, where models must rely on internal signals (e.g., inherent self-consistency, entropy, or confidence) to generate rewards for themselves (Grandvalet & Bengio, 2004; Lee et al., 2013; Zuo et al., 2025; Shafayat et al., 2025; Li et al., 2025b).

The fundamental flaw in relying on internal signals is not merely that they are initially noisy or biased, but that the learning process itself actively degrades the quality of the reward signal over time (Liang et al., 2024). By rewarding conformity to its self-confirmation, the model systematically eliminates the solution diversity (Lee et al., 2024). This creates a degenerative feedback loop: a progressively narrower and more biased policy generates an increasingly impoverished reward signal,

*Work done during Yujun’s Internship at Tencent AI Lab.

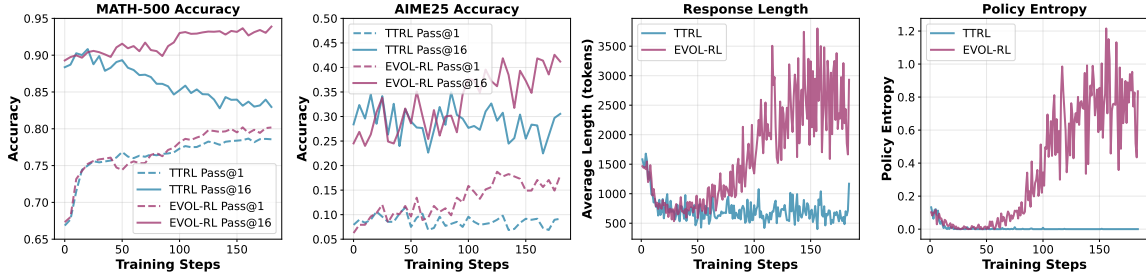


Figure 1: TTRL’s entropy collapse vs. EVOL-RL’s diversity preservation on Qwen3-4B-Base (trained label-free on MATH-500). Majority-only TTRL drives $\text{pass}@n > 1$ down, shortens reasoning, and collapses entropy, whereas EVOL-RL improves accuracy, sustains reasoning diversity.

which in turn accelerates the policy’s collapse into a low-entropy state (Ding et al., 2025; Liang et al., 2024; 2025b). Similar dynamics are well known in RL and self-training when entropy regularization or external supervision is absent (Haarnoja et al., 2018). Recent studies also show that training on self-generated data can harm diversity over time (Shumailov et al., 2024) and eventually lead to collapse. Figure 1 illustrates this phenomenon in reasoning: under traditional Test-Time Reinforcement Learning (TTRL) (Zuo et al., 2025), $\text{pass}@1$ may rise but $\text{pass}@n$ drops, while response length and complexity steadily decline, indicating that the model fails to evolve.

In this paper, we ground LLM evolving in the simple rule behind biological evolution: *variation* creates new candidates; *selection* keeps what works. Existing methods effectively implement only the *selection* half of evolution, driving the population toward whatever the model already believes. This majority-only (or entropy minimization, confidence maximization) reinforcement amplifies existing biases and often leads entropy collapse and shrinking response diversity, as shown above. Our formulation restores the full evolutionary loop: we pair *selection*, which stabilizes optimization by keeping high-quality solutions, with *variation*, which explicitly promotes novelty and sustains exploration. This idea is deeply rooted in decades of evolutionary computation research, including genetic algorithms (Holland, 1992; Eiben & Smith, 2015), novelty search (Lehman & Stanley, 2011), and quality–diversity (QD) methods such as MAP-Elites (Pugh et al., 2016), which collectively show that diversity preservation is essential for avoiding collapse and enabling robust, long-term progress.

Hence, we propose *Evolution-Oriented and Label-free Reinforcement Learning (EVOL-RL)*, a simple objective that combines a stabilizing *selection* signal with an explicit *variation* incentive. Concretely, EVOL-RL retains the majority-voted answer as the anchor for stability, but adds a novelty-aware reward that scores each sampled solution by how different its reasoning is from other concurrently generated responses (semantic similarity of their reasoning traces). This majority-for-stability + novelty-for-exploration rule mirrors the variation–selection principle: *selection prevents drift; novelty prevents collapse*. As demonstrated in Figure 1, EVOL-RL successfully averts all symptoms of diversity collapse, fostering a healthy equilibrium between refining known solutions and discovering new ones. This balanced approach translates into substantial performance gains, especially in out-of-domain generalization. For instance, after training on AIME24, EVOL-RL elevates the Qwen3-4B-base model’s $\text{pass}@1$ accuracy on the AIME25 benchmark from 4.6% (TTRL) to 16.4%, while more than doubling the $\text{pass}@16$ accuracy from 18.5% to 37.9%.

Contributions. (1) We diagnose why majority-only objectives shrink exploration during label-free training and formalize their link to entropy collapse on reasoning tasks. (2) We provide a new perspective on label-free learning by framing it as an evolutionary system. This view allows us to diagnose diversity collapse as a form of premature convergence and solve it by applying the core evolutionary principle of balancing selection with variation. (3) We design a practical novelty-aware reward that complements majority selection and enables stable, label-free improvement. Across math benchmarks, EVOL-RL reverses the $\text{pass}@n$ decline, maintains longer and more informative chains of thought, and improves out-of-domain accuracy, while remaining simple to implement. (4) We deliver state-of-the-art results in unsupervised RL training, demonstrating that

EVOL-RL achieves significant out-of-domain generalization gains where prior methods fail, such as more than tripling pass@1 accuracy and doubling pass@16 accuracy on AIME25 benchmark. (5) We provide a theoretical analysis of entropy stabilization in Appendix D. We formally prove that while a correctness-only objective allows the optimal policy to collapse onto a single response, our novelty-augmented objective *guarantees* that the optimal policy must distribute probability mass across multiple correct modes, providing a rigorous foundation for the method’s stability.

2 Related Works

Enhancing Reasoning in LLMs. Significant progress in LLM reasoning has been driven by RLVR (Jaech et al., 2024; Guo et al., 2025; Yang et al., 2025; Yu et al., 2025; Xiong et al., 2025; Dai et al., 2025b; Wang et al., 2025c; Zhuang et al., 2025), which fine-tunes models using RL on tasks where an automated verifier can confirm the correctness of the final answer, such as mathematics and coding (Zeng et al., 2025; Wang et al., 2025a;b; Cui et al., 2025; Huang et al., 2025; Dai et al., 2025a; Zheng et al., 2025b; Zhou et al., 2025b; Zheng et al., 2025a; Fang et al., 2025; Liu et al., 2025b). While highly effective, the reliance of RLVR on external verifiers restricts its applicability to domains with deterministic, easily checkable solutions (Zhao et al., 2025c;a; Zhou et al., 2025a; 2024; Liang et al., 2025a). Our work contributes to the effort of improving reasoning in more general domains where such verifiers are unavailable.

Label-Free Adaptation and Self-Improvement. To overcome the limitations of verifiers and adapt to new data distributions, researchers have focused on label-free learning methods. These approaches primarily fall into two categories. One line of research derives rewards from the model’s intrinsic confidence, training the model to become more "certain" by rewarding low-entropy or self-consistent outputs (Prabhudesai et al., 2025; Agarwal et al., 2025; Zhao et al., 2025b; Zhang et al., 2025b; Shafayat et al., 2025; Chung et al., 2025; Zhang et al., 2025a). The other prominent paradigm, which we directly address, bootstraps supervision from majority, exemplified by TTRL (Zuo et al., 2025). While empirically powerful, we identify a critical flaw in the majority-driven approach: it suppresses solution diversity and actively punishes correct but non-mainstream reasoning, leading to entropy collapse. Crucially, generic strategies like adding entropy loss or clip-high (Cui et al., 2025; Park et al., 2025) are insufficient to escape this "majority trap." Instead, we propose a *directional novelty reward* that re-ranks credit based on semantic uniqueness. This fully label-free approach fundamentally redesigns the reward signal, distinguishing our work from methods that separate trained evaluators (Li et al., 2025a; Pang et al., 2023) or simple exploration adjustments (Liu et al., 2025a).

3 Method

Our approach is illustrated in Figure 2. which uses Group Relative Policy Optimization (GRPO) (Shao et al., 2024) as its optimization algorithm, but guides it with a novel reward function that explicitly balances majority with novelty.

3.1 Optimization with GRPO

GRPO is a policy-gradient algorithm designed for fine-tuning LLMs without a separate value function. Its central idea is to evaluate each sampled response relative to a group of its peers generated for the same prompt. This relative evaluation is then used to update the policy with a PPO-style clipped objective, regularized by a KL penalty to ensure stable learning.

For a prompt \mathbf{q} , a policy LLM $\pi_{\theta_{\text{old}}}$ generates a group of G responses $\{\mathbf{o}_1, \dots, \mathbf{o}_G\}$. Each response \mathbf{o}_i receives a scalar reward r_i . Rewards within the group are normalized with a z-score to obtain a response-level advantage:

$$\hat{A}_i = \frac{r_i - \text{mean}(r_1, \dots, r_G)}{\text{std}(r_1, \dots, r_G)},$$

The policy is optimized with a clipped surrogate objective:

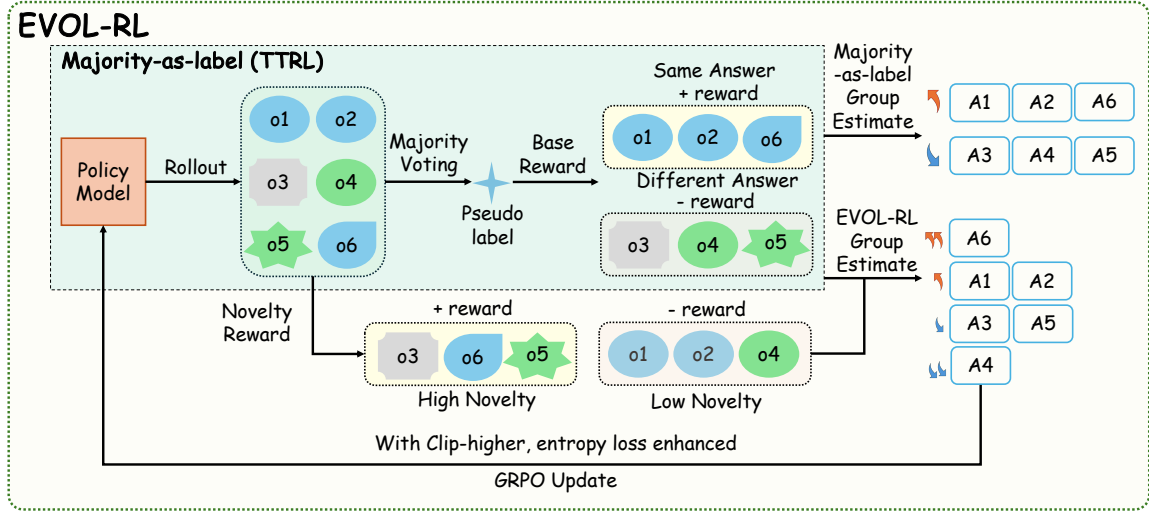


Figure 2: An overview of the EVOL-RL framework. For each prompt, the policy generates multiple responses. These are grouped by their final answer to identify the majority group. A novelty score is then computed for each response based on its semantic dissimilarity to others. Finally, a reward is assigned based on both majority (selection) and novelty (variation), guiding the policy update via GRPO. In the illustration, colors group responses by their final answer, while different marker shapes indicate semantically distinct reasoning paths.

$$\frac{1}{G} \sum_{i=1}^G \frac{1}{|o_i|} \sum_{t=1}^{|o_i|} \min \left\{ \frac{\pi_{\theta}(o_{i,t} | \mathbf{q}, \mathbf{o}_{i,<t})}{\pi_{\theta_{\text{old}}}(o_{i,t} | \mathbf{q}, \mathbf{o}_{i,<t})} \hat{A}_{i,t}, \text{clip} \left(\frac{\pi_{\theta}(o_{i,t} | \mathbf{q}, \mathbf{o}_{i,<t})}{\pi_{\theta_{\text{old}}}(o_{i,t} | \mathbf{q}, \mathbf{o}_{i,<t})}, 1 - \epsilon_{\text{low}}, 1 + \epsilon_{\text{high}} \right) \hat{A}_{i,t} \right\} \quad (1)$$

3.2 Reward Design: Implementing Selection and Variation

Our reward design directly implements the principles of selection and variation to counteract diversity collapse. Selection, based on correctness via majority vote, provides a stable signal to prevent the policy from drifting. Variation, driven by semantic novelty, provides the exploratory pressure needed to maintain a diverse set of reasoning strategies.

A key design choice is that the novelty incentive is applied strategically to all solutions—both those that agree with the majority and those that do not. For majority-aligned solutions, rewarding novelty encourages the model to discover multiple valid reasoning paths to the correct answer, directly fighting the decline in pass@n performance. For minority solutions, rewarding novelty is crucial for escaping local optima. It discourages policy collapse into a few high-frequency failure modes and instead incentivizes exploration of the broader reasoning space, which is essential for increasing the probability of discovering a previously inaccessible, correct solution path. This integration transforms the learning process: it not only mitigates diversity collapse in the current task but also aligns with the goals of continual learning. By preserving multiple reasoning modes while anchoring to a correct solution, EVOL-RL avoids forgetting potentially useful strategies and retains knowledge diversity for future tasks. Thus, training under EVOL-RL becomes not only an optimization for present performance but also a proactive investment in future adaptability.

Reward Formulation. For each prompt, the policy samples G responses $\{o_i\}_{i=1}^G$. Each response is scored on three criteria:

1. Validity: The response must provide a numeric final answer in a `\boxed{\cdot}` format. Responses that fail this check are deemed invalid.

2. Majority (Selection): A binary label $y_i \in \{+1, -1\}$ is assigned based on whether a response’s answer matches the majority-voted answer from the valid responses. This serves as our selection signal.

3. Novelty (Variation): We compute embeddings for the reasoning part of each response to form a cosine similarity matrix. For each response o_i , we calculate its mean similarity \bar{s}_i to other responses in the same group (i.e., either majority or minority) and its maximum similarity m_i to any other response in the entire batch. The mean similarity is calculated on an intra-group basis because the majority and minority solutions are often semantically distant; a global mean would be dominated by this gap, obscuring the finer-grained variations among peer solutions within the majority group. The novelty score is:

$$u_i = 1 - (\alpha \bar{s}_i + (1 - \alpha) m_i), \quad \alpha \in (\text{default } 0.5).$$

This score is designed to penalize two distinct forms of redundancy: a high \bar{s}_i indicates conformity to the group’s semantic average, while a high m_i flags near-duplication of another specific response. The score promotes both local and global diversity. Finally, we min-max normalize the scores $\{u_i\}$ separately within the majority and minority groups to get \tilde{u}_i . This intra-group normalization is crucial, as it ensures that novelty is measured relative to one’s direct peers, allowing for a fair comparison of diversity within each group.

Final Reward Mapping. We map the majority label and normalized novelty score into non-overlapping reward bands. This ensures that the selection signal from the majority vote is always prioritized, while novelty refines the reward within each group:

$$r_i = \begin{cases} -1, & \text{if invalid;} \\ 0.5 + 0.5 \tilde{u}_i \in [0.5, 1], & \text{if } y_i = +1; \\ -1 + 0.5 \tilde{u}_i \in [-1, -0.5], & \text{if } y_i = -1. \end{cases}$$

Critically, this structure guarantees that any majority solution, regardless of its novelty, receives a higher reward than any minority solution. This maintains a strong pressure towards correctness. More details about the reward implementation are presented in Appendix A.4

Supporting Mechanisms. To further reinforce this reward design, we employ two complementary mechanisms. First, within the GRPO objective (Eq. 1), we use an asymmetric clipping range ($\epsilon_{\text{high}} > \epsilon_{\text{low}}$) (Yu et al., 2025). This allows promising and novel solutions with high advantages to receive larger gradient updates, preventing them from being prematurely clipped. Second, we add a token-level entropy regularizer to maintain diversity during the initial generation process:

$$\mathcal{L}_{\text{ent}}(\theta) = -\lambda_{\text{ent}} \mathbb{E}_{o \sim \pi_\theta} \left[\frac{1}{|o|} \sum_{t=1}^{|o|} H(\pi_\theta(\cdot \mid o_{<t}, x)) \right], \quad (2)$$

$$H(p) = - \sum_v p(v) \log p(v).$$

The total objective, $\mathcal{L}_{\text{total}} = \mathcal{L}_{\text{GRPO}} + \mathcal{L}_{\text{ent}}$, thus directs learning toward semantically distinct, high-quality responses while maintaining a diverse population of solutions.

3.3 How EVOL-RL Avoids Collapse Through an Evolutionary Analogy.

EVOL-RL avoids this failure mode by mirroring biological evolution, which balances a stabilizing Selection pressure with a dynamic Variation mechanism. The majority vote acts as our Selection pressure, providing a crucial anchor to correctness. By itself, however, this would lead to a uniform population of solutions, vulnerable to collapse, much like a species with no genetic diversity is vulnerable to a single disease.

To prevent this, our three-part Variation strategy creates a robust exploratory dynamic. The entropy regularizer acts like a higher "mutation rate," ensuring a constant supply of diverse solutions

for the system to work with. The novelty reward then provides directional pressure to this variation, giving a “survival bonus” to solutions that are semantically distinct from their peers. Finally, asymmetric clipping ensures that when a highly beneficial “mutation”—a rare, novel, and correct solution—appears, its strong learning signal is fully preserved for the next generation.

This design makes a collapsed state inherently unstable. In a uniform population, any novel solution receives a higher reward, forcing the algorithm to shift probability toward diverse solutions.

Theoretical Support. We formally validate this evolutionary intuition in Appendix D. We prove that while a correctness-only objective (J_0) admits degenerate optimal policies that collapse onto a single solution, our diversity-augmented objective (J_λ) alters the optimization landscape. Under mild assumptions, the global maximizer of our objective is theoretically guaranteed to spread probability mass across all correct reasoning modes (Theorem 1), thereby preventing the entropy collapse observed in standard self-training.

4 Experiments

4.1 Experimental Setup

Benchmarks. To test our method at scale, we use the large, standard **MATH training set (MATH-TRAIN)** (Hendrycks et al., 2021). We also follow the TTRL (Zuo et al., 2025) by training on two much smaller test sets: the general-purpose **MATH-500** and the competition-level **AIME24** (Li et al., 2024). This comprehensive setup allows us to validate EVOL-RL’s versatility across both large-scale and specialized training conditions. Critically, during all training runs, we use only the problem statements, without any ground-truth labels or solutions. For evaluation, we assess the performance of our trained models on a diverse set of five benchmarks to measure both in-domain and out-of-domain generalization. The evaluation suite includes **AIME24**, **AIME25**, **MATH500**, **AMC** (Li et al., 2024), and **GPQA-Diamond (GPQA)** (Rein et al., 2024). Detailed training configuration can be found in Appendix A. Furthermore, we provide additional experimental results on OctoThinker-8B-Hybrid-Base in Appendix B.1. More baseline comparisons, including Entropy Minimization (Agarwal et al., 2025) and Self-Consistency (Wang et al., 2023; Huang et al., 2023), are presented in Appendix B.2. The analysis of the extra time incurred by embedding computation and similarity measurement has been moved to Appendix B.5. A case study in Appendix B.6 shows that embedding similarity reliably captures differences in reasoning paths.

4.2 Main Results

The main results of our experiments are summarized in Table 1. We highlight four key findings that demonstrate the superiority of EVOL-RL over the majority-only TTRL baseline.

EVOL-RL Enhances Both Pass@1 and Pass@16 Performance. Across all experimental settings, EVOL-RL consistently and substantially improves ‘pass@16’ performance over TTRL, with gains frequently exceeding 20 percentage points on the most challenging benchmarks (e.g., +24.2% on AIME24 for the 4B model). EVOL-RL also delivers more consistent and substantial improvements to pass@1 accuracy than TTRL. This demonstrates that our method strengthens not only the model’s single-shot accuracy but also its ability to explore through multiple attempts.

Consistent Improvements Across Model Scales and Training Data Sizes. The benefits of EVOL-RL are robust across both the 4B and 8B model scales, and critically, across training datasets of vastly different sizes. The performance improvements hold true whether training on the large-scale MATH-TRAIN set or the smaller, more specialized MATH-500 and AIME24 sets. This suggests that the underlying mechanism—balancing a majority anchor with novelty-driven rewards—is a fundamental improvement that scales effectively with both model capacity and data volume.

Strong Cross-Difficulty Robustness EVOL-RL demonstrates powerful generalization, learning abstract reasoning skills that transfer effectively across different mathematical domains. A powerful example is seen with the 4B model: when trained exclusively on MATH-500, its pass@16 perfor-

Table 1: Comparison of models trained with TTRL and EVOL-RL. Each cell shows pass@1/pass@16 (averaged on 32 rollouts). Δ uses red (+) for positive and blue for negative values, showing the difference between w/EVOL-RL and w/TTRL.

Training Dataset	Model	MATH	AIME24	AIME25	AMC	GPQA
Qwen3-4B-Base						
–	Base Model	67.4/89.6	10.0/32.4	5.5/30.0	39.3/75.2	34.4/85.6
MATH-TRAIN	w/TTRL	75.4/86.9	12.1/23.2	6.8/28.6	42.5/75.2	36.5/81.4
	w/EVOL-RL	80.0/93.3	20.7/47.6	17.5/39.9	51.4/80.3	37.2/88.7
	Δ	+4.6/+6.4	+8.6/+24.4	+10.7/+11.3	+8.9/+5.1	+0.7/+7.3
MATH-500	w/TTRL	79.3/83.2	10.0/28.0	7.2/29.9	47.6/72.0	36.2/75.9
	w/EVOL-RL	79.8/93.8	19.0/43.2	16.1/41.9	50.3/82.2	38.8/89.1
	Δ	+0.5/+10.6	+9.0/+15.2	+8.9/+12.0	+2.7/+10.2	+2.6/+13.2
AIME24	w/TTRL	73.8/84.5	16.7/16.7	4.6/18.5	43.6/65.8	35.1/73.5
	w/EVOL-RL	79.6/93.6	20.6/40.9	17.1/42.0	49.9/80.9	38.0/87.8
	Δ	+5.8/+9.1	+3.9/+24.2	+12.5/+23.5	+6.3/+15.1	+2.9/+14.3
Qwen3-8B-Base						
–	Base Model	63.6/91.5	12.0/39.4	8.2/30.8	38.7/77.6	34.9/88.0
MATH-TRAIN	w/TTRL	81.1/91.1	16.7/37.6	15.6/35.9	53.6/74.0	38.1/77.1
	w/EVOL-RL	83.6/94.1	26.0/51.7	21.6/43.1	55.5/86.1	43.5/88.1
	Δ	+2.5/+3.0	+9.3/+14.1	+6.0/+7.2	+1.9/+12.1	+5.4/+11.0
MATH-500	w/TTRL	85.7/91.9	17.7/40.1	16.5/34.3	51.1/79.1	43.5/84.0
	w/EVOL-RL	84.7/95.1	24.1/49.5	20.2/44.4	58.8/86.0	43.9/92.2
	Δ	-1.0/+3.2	+6.4/+9.4	+3.7/+10.1	+7.7/+6.9	+0.4/+8.2
AIME24	w/TTRL	76.8/86.2	20.0/20.0	11.4/25.4	49.5/69.1	38.3/74.7
	w/EVOL-RL	83.1/94.2	25.4/38.1	16.5/34.7	54.4/85.8	45.2/90.0
	Δ	+6.3/+8.0	+5.4/+18.1	+5.1/+9.3	+4.9/+16.7	+6.9/+15.3

mance on AIME24 and AIME25 is nearly identical to the performance achieved when training on AIME24 directly, confirming that EVOL-RL learns fundamental skills rather than simply overfitting. This effect is further amplified by scale; for the 8B model, training on the large MATH-TRAIN dataset yields pass@1 performance on AIME24 (26.0%) and AIME25 (21.6%) that is far superior to training on AIME24 directly (25.4% and 16.5% respectively). This indicates that EVOL-RL effectively leverages both specialized and large-scale data to build fundamental and transferable reasoning abilities.

Generalization on Non-Mathematical Reasoning Tasks. The advantages of EVOL-RL extend beyond the domain of mathematics. On the GPQA benchmark, where TTRL consistently causes pass@16 performance to degrade compared to the base model, EVOL-RL reliably recovers and surpasses the base model. Across all training configurations, it achieves gains of +7 to +15 % in pass@16 over TTRL, indicating that our diversity-preserving reward mechanism fosters a more generalizable reasoning ability that transfers effectively across different domains.

4.3 Ablation Study

Setup. We conduct an ablation study on EVOL-RL-trained models on Qwen3-4B-Base. EVOL-RL introduces three key modifications compared to the TTRL baseline: (i) the novelty-aware re-

Table 2: Performance of Qwen3-4B-Base with EVOL-RL and its ablations. Each cell reports pass@1/pass@16 accuracy.

Training Dataset	Model	MATH	AIME24	AIME25	AMC	GPQA
MATH-500	w/EVOL-RL	79.8/93.8	19.0/43.2	16.1/41.9	50.3/82.2	38.8/89.1
	-ClipHigh	75.1/91.8	12.2/31.8	11.4/31.3	42.7/73.9	32.3/81.8
	-Ent	79.5/93.4	18.3/38.5	14.7/34.3	48.3/78.6	38.6/87.0
	-ClipHigh-Ent	76.3/92.6	12.8/38.8	12.5/37.4	46.2/77.4	35.6/88.8
	-Novelty Reward	79.3/88.7	12.1/27.0	11.1/34.8	47.6/73.3	37.9/81.4
AIME24	w/EVOL-RL	79.6/93.6	20.6/40.9	17.1/42.0	49.9/80.9	38.0/87.8
	-ClipHigh	74.1/89.4	14.1/26.7	8.1/31.1	44.6/73.2	35.3/81.5
	-Ent	66.7/89.8	10.0/31.4	6.6/27.8	38.7/74.2	34.0/86.2
	-ClipHigh-Ent	75.3/89.0	16.6/26.9	9.2/32.2	45.8/71.2	37.1/82.0
	-Novelty Reward	79.4/93.0	17.7/35.6	15.9/37.4	48.8/79.6	37.9/87.1

ward function, (ii) a rollout entropy regularizer to encourage exploration, and (iii) an asymmetric PPO clipping window (higher "ClipHigh") to better preserve learning signals from high-reward samples. We systematically remove these components one at a time ("-Novelty Reward", "-Ent", "-ClipHigh") or in combination. The results are reported in Table 2.

The Critical Role of Novelty on Easier Datasets. The importance of the novelty reward is most evident when the model is trained on the MATH-500 dataset. Removing it causes the largest performance degradation in pass@16, especially on the more difficult, out-of-domain AIME24/25. This is because on a dataset with lower complexity, a majority-only approach can quickly cause the model to lock into a single, repetitive reasoning template. Our novelty reward prevents this template lock-in and promotes generalizable skills.

Exploration Mechanisms as Critical Enablers on Harder Tasks. On more challenging datasets like AIME24, where the inherent problem difficulty naturally induces a higher baseline of exploration, the other two components become more critical. In this setting, removing the entropy regularizer or the asymmetric clipping consistently lowers pass@16 performance on AIME-style problems. These mechanisms act as crucial enablers for the novelty reward: the entropy regularizer ensures a rich and continuous supply of varied reasoning paths for the novelty selector to act upon, while the higher clipping threshold preserves the full learning signal from rare but high-value solutions.

4.4 Training Dynamics: How EVOL-RL Escapes Entropy Collapse

To understand the reasons for EVOL-RL’s better performance, we analyze its training dynamics in comparison to TTRL in a label-free setting, as shown in Figure 3. An analysis of the training dynamics for the 8B models is presented in Appendix B.4.

Stage 1: Initial Collapse Under Majority Signal. Across all three training settings, a consistent initial dynamic unfolds: both EVOL-RL and TTRL show a sharp drop in policy entropy and average response length. This initial phase demonstrates the powerful homogenizing effect of the majority-driven reward, which quickly pushes both models toward short, high-frequency response templates. For TTRL, this collapsed state proves to be permanent; it remains trapped in this low-entropy, low-complexity state for the duration of the training run, regardless of the dataset’s scale or difficulty.

Stage 2: The Evolving Point and Coordinated Recovery. Following the initial collapse, the training dynamics reveal a crucial divergence centered around a distinct "evolving point". Before this point, EVOL-RL’s trajectory is nearly indistinguishable from TTRL’s; both models exhibit similar performance values and trends, dominated by the majority signal. However, a clear inflection point consistently emerges for EVOL-RL, after which its performance rapidly improves. While

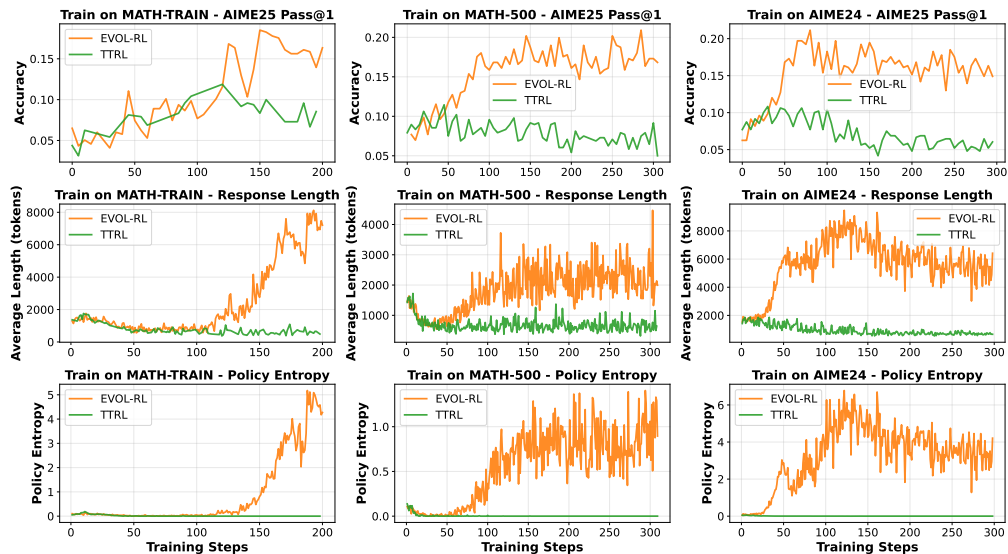


Figure 3: Training dynamics for EVOL-RL and TTRL. **Left:** models trained on *MATH-TRAIN*. **Middle:** models trained on *MATH-500*. **Right:** models trained on *AIME24*. Each panel plots, over training steps, (i) Pass@1 on *AIME25*, (ii) average response length on the training set, and (iii) policy entropy on the training set.

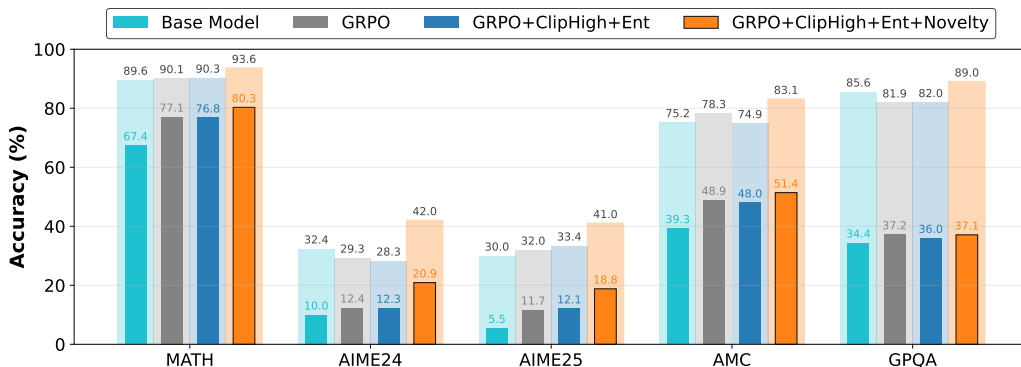


Figure 4: Performance of EVOL-RL's exploration-enhancing components when applied to a standard supervised GRPO baseline. The Qwen3-4B-Base model is trained on the *MATH* training set (Hendrycks et al., 2021) with a ground-truth verifier (RLVR).

the exact timing of this "evolving point" varies across datasets, its appearance is a robust feature of our method. After this "evolving point", EVOL-RL enters a recovery phase characterized by a sustained and coordinated rise across all key metrics: policy entropy breaks away from near-zero values, average response length increases, and out-of-domain accuracy steadily climbs. This coordinated recovery allows the model to reach a new, significantly higher performance plateau where it eventually stabilizes, demonstrating its ability to break free from the majority trap.

EVOL-RL's ability to escape the collapsed state comes from the synergy of its three core components. The entropy regularizer ensures a continuous supply of diverse rollouts, preventing the initial search space from becoming completely uniform. The asymmetric clipping preserves the full gradient signal from the rare but high-value "majority-and-novel" samples that are crucial in the early training phase. Finally, the novelty reward acts as a selection pressure, consistently re-ranking credit within the majority group to favor these distinct solutions over their near-duplicate peers.

Table 3: Generalization performance of the Qwen3-8B-Base model on broader reasoning benchmarks after label-free training on MATH-TRAIN.

Model	MMLU-Pro		SuperGPQA		BBEH	
	Pass@1	Pass@4	Pass@1	Pass@4	Pass@1	Pass@4
Qwen3-8B-Base	47.3	74.5	26.5	54.1	10.4	24.0
w/TTRL	53.4	73.9	29.7	53.3	12.1	24.1
w/EVOL-RL	55.3	78.5	30.2	57.0	11.5	24.9

4.5 EVOL-RL Components Also Strengthen Supervised GRPO (RLVR)

Setup. We apply EVOL-RL’s three exploration-enhancing ingredients to a standard supervised GRPO baseline trained on *MATH* training set (Hendrycks et al., 2021) with a ground-truth verifier (RLVR) for two epochs. Figure 4 reports the results.

The primary finding is that the three components are still synergistic, with their full combination yielding the most significant and consistent performance improvements. This complete configuration, GRPO+ClipHigh+Ent+Novelty, boosts pass@16 accuracy by 7% to 12% on the challenging out-of-domain AIME24 and AIME25 benchmarks. Crucially, these gains are achieved while also improving pass@1 accuracy, demonstrating that the mechanisms enhance multi-path reliability without sacrificing single-shot performance. This robust improvement extends across all evaluation benchmarks, including the cross-domain GPQA task, demonstrating the great potential of variation reward in a broader context.

4.6 Generalization to Broader Reasoning Benchmarks

To assess whether the reasoning skills enhanced by our method on mathematical data are fundamental and transferable, we evaluate our models on a suite of broader, non-mathematical reasoning benchmarks. After training the Qwen3-8B-Base model on the MATH-TRAIN dataset in a label-free setting, we measure its performance on **MMLU-Pro** (Wang et al., 2024), **SuperGPQA** (Team et al., 2025), and **BBEH** (Kazemi et al., 2025). The results, presented in Table 3, demonstrate that EVOL-RL fosters a more generalizable reasoning ability compared to TTRL.

A contrasting pattern emerges between the two methods. While TTRL shows clear improvements over the base model on pass@1 accuracy, its effect on pass@4 is less consistent, falling slightly below the base model’s performance on SuperGPQA and BBEH. This pattern is consistent with our findings on the mathematical reasoning tasks, where the narrow focus of the consensus-only objective can hurt multi-path reliability. In contrast, EVOL-RL demonstrates a more robustly positive transfer of skills, improving upon both the base model and TTRL across pass@1 and pass@4 metrics. For example, on MMLU-Pro, EVOL-RL achieves a pass@4 score of 78.5%, a clear improvement over TTRL’s 73.9%. This indicates that our principle of encouraging diverse reasoning helps the model learn more fundamental skills that generalize effectively beyond mathematics.

5 Conclusion

In this work, we diagnose the entropy collapse, a critical failure mode in LLM evolving where majority-only rewards suppress solution diversity and harm generalization. To solve this, we propose EVOL-RL, a framework that balances the stability of majority-vote selection with an explicit variation incentive that rewards semantic novelty. Our experiments demonstrate that EVOL-RL successfully prevents collapse by maintaining policy entropy and reasoning complexity, which translates into substantial performance gains on both in-domain and out-of-domain benchmarks. By anchoring learning to a stable majority signal while simultaneously encouraging exploration, EVOL-RL offers a robust and practical methodology for enabling LLMs to continuously and autonomously evolve without external labels.

References

- Shivam Agarwal, Zimin Zhang, Lifan Yuan, Jiawei Han, and Hao Peng. The unreasonable effectiveness of entropy minimization in llm reasoning. *arXiv preprint arXiv:2505.15134*, 2025.
- John Joon Young Chung, Vishakh Padmakumar, Melissa Roemmele, Yuqian Sun, and Max Kreminski. Modifying large language model post-training for diverse creative writing. *arXiv preprint arXiv:2503.17126*, 2025.
- Ganqu Cui, Yuchen Zhang, Jiacheng Chen, Lifan Yuan, Zhi Wang, Yuxin Zuo, Haozhan Li, Yuchen Fan, Huayu Chen, Weize Chen, et al. The entropy mechanism of reinforcement learning for reasoning language models. *arXiv preprint arXiv:2505.22617*, 2025.
- Runpeng Dai, Linfeng Song, Haolin Liu, Zhenwen Liang, Dian Yu, Haitao Mi, Zhaopeng Tu, Rui Liu, Tong Zheng, Hongtu Zhu, et al. Cde: Curiosity-driven exploration for efficient reinforcement learning in large language models. *arXiv preprint arXiv:2509.09675*, 2025a.
- Runpeng Dai, Tong Zheng, Run Yang, Kaixian Yu, and Hongtu Zhu. R1-re: Cross-domain relation extraction with rlvr. *arXiv preprint arXiv:2507.04642*, 2025b.
- Mucong Ding, Souradip Chakraborty, Vibhu Agrawal, Zora Che, Chenghao Deng, Alec Koppel, Mengdi Wang, Dinesh Manocha, Amrit Singh Bedi, and Furong Huang. SAIL: Self-improving efficient online alignment of large language models, 2025. URL <https://openreview.net/forum?id=02kZwCo0C3>.
- Agoston E Eiben and James E Smith. *Introduction to evolutionary computing*. Springer, 2015.
- Wenkai Fang, Shunyu Liu, Yang Zhou, Kongcheng Zhang, Tongya Zheng, Kaixuan Chen, Mingli Song, and Dacheng Tao. Serl: Self-play reinforcement learning for large language models with limited data. *arXiv preprint arXiv:2505.20347*, 2025.
- Yves Grandvalet and Yoshua Bengio. Semi-supervised learning by entropy minimization. *Advances in neural information processing systems*, 17, 2004.
- Daya Guo, Dejian Yang, Haowei Zhang, Junxiao Song, Ruoyu Zhang, Runxin Xu, Qihao Zhu, Shirong Ma, Peiyi Wang, Xiao Bi, et al. Deepseek-r1: Incentivizing reasoning capability in llms via reinforcement learning. *arXiv preprint arXiv:2501.12948*, 2025.
- Tuomas Haarnoja, Aurick Zhou, Pieter Abbeel, and Sergey Levine. Soft actor-critic: Off-policy maximum entropy deep reinforcement learning with a stochastic actor. In *International conference on machine learning*, pp. 1861–1870. Pmlr, 2018.
- Dan Hendrycks, Collin Burns, Saurav Kadavath, Akul Arora, Steven Basart, Eric Tang, Dawn Song, and Jacob Steinhardt. Measuring mathematical problem solving with the math dataset. *arXiv preprint arXiv:2103.03874*, 2021.
- John H Holland. *Adaptation in natural and artificial systems: an introductory analysis with applications to biology, control, and artificial intelligence*. MIT press, 1992.
- Chengsong Huang, Wenhao Yu, Xiaoyang Wang, Hongming Zhang, Zongxia Li, Ruosen Li, Jiaxin Huang, Haitao Mi, and Dong Yu. R-zero: Self-evolving reasoning llm from zero data. *arXiv preprint arXiv:2508.05004*, 2025.
- Jiaxin Huang, Shixiang Gu, Le Hou, Yuexin Wu, Xuezhi Wang, Hongkun Yu, and Jiawei Han. Large language models can self-improve. In *Proceedings of the 2023 conference on empirical methods in natural language processing*, pp. 1051–1068, 2023.
- Aaron Jaech, Adam Kalai, Adam Lerer, Adam Richardson, Ahmed El-Kishky, Aiden Low, Alec Helyar, Aleksander Madry, Alex Beutel, Alex Carney, et al. Openai o1 system card. *arXiv preprint arXiv:2412.16720*, 2024.

- Mehran Kazemi, Bahare Fatemi, Hritik Bansal, John Palowitch, Chrysovalantis Anastasiou, San-
ket Vaibhav Mehta, Lalit K. Jain, Virginia Aglietti, Disha Jindal, Peter Chen, Nishanth Dikkala,
Gladys Tyen, Xin Liu, Uri Shalit, Silvia Chiappa, Kate Olszewska, Yi Tay, Vinh Q. Tran, Quoc V.
Le, and Orhan Firat. Big-bench extra hard, 2025. URL <https://arxiv.org/abs/2502.19187>.
- Dong-Hyun Lee et al. Pseudo-label: The simple and efficient semi-supervised learning method for
deep neural networks. In *Workshop on challenges in representation learning, ICML*, volume 3, pp.
896. Atlanta, 2013.
- Sangkyu Lee, Sungdong Kim, Ashkan Yousefpour, Minjoon Seo, Kang Min Yoo, and Young-
jae Yu. Aligning large language models by on-policy self-judgment. In Lun-Wei Ku, Andre
Martins, and Vivek Srikumar (eds.), *Proceedings of the 62nd Annual Meeting of the Association
for Computational Linguistics (Volume 1: Long Papers)*, pp. 11442–11459, Bangkok, Thailand, Au-
gust 2024. Association for Computational Linguistics. doi: 10.18653/v1/2024.acl-long.617. URL
<https://aclanthology.org/2024.acl-long.617/>.
- Joel Lehman and Kenneth O Stanley. Abandoning objectives: Evolution through the search for
novelty alone. *Evolutionary computation*, 19(2):189–223, 2011.
- Jia Li, Edward Beeching, Lewis Tunstall, Ben Lipkin, Roman Soletskyi, Shengyi Huang, Kashif
Rasul, Longhui Yu, Albert Q Jiang, Ziju Shen, et al. Numinamath: The largest public dataset in
ai4maths with 860k pairs of competition math problems and solutions. *Hugging Face repository*,
13(9):9, 2024.
- Tianjian Li, Yiming Zhang, Ping Yu, Swarnadeep Saha, Daniel Khashabi, Jason Weston, Jack Lan-
chantin, and Tianlu Wang. Jointly reinforcing diversity and quality in language model genera-
tions. *arXiv preprint arXiv:2509.02534*, 2025a.
- Zongxia Li, Wenhao Yu, Chengsong Huang, Rui Liu, Zhenwen Liang, Fuxiao Liu, Jingxi Che, Dian
Yu, Jordan Boyd-Graber, Haitao Mi, et al. Self-rewarding vision-language model via reasoning
decomposition. *arXiv preprint arXiv:2508.19652*, 2025b.
- Xun Liang, Shichao Song, Zifan Zheng, Hanyu Wang, Qingchen Yu, Xunkai Li, Rong-Hua Li,
Yi Wang, Zhonghao Wang, Feiyu Xiong, and Zhiyu Li. Internal consistency and self-feedback
in large language models: A survey, 2024. URL <https://arxiv.org/abs/2407.14507>.
- Zhenwen Liang, Ruosen Li, Yujun Zhou, Linfeng Song, Dian Yu, Xinya Du, Haitao Mi, and Dong
Yu. Clue: Non-parametric verification from experience via hidden-state clustering. *arXiv preprint
arXiv:2510.01591*, 2025a.
- Zhenwen Liang, Sidi Lu, Wenhao Yu, Kishan Panaganti, Yujun Zhou, Haitao Mi, and Dong Yu. Can
llms guide their own exploration? gradient-guided reinforcement learning for llm reasoning.
arXiv preprint arXiv:2512.15687, 2025b.
- Jia Liu, Changyi He, Yingqiao Lin, Mingmin Yang, Feiyang Shen, ShaoGuo Liu, and TingTing Gao.
Ettrl: Balancing exploration and exploitation in llm test-time reinforcement learning via entropy
mechanism. *arXiv preprint arXiv:2508.11356*, 2025a.
- Rui Liu, Dian Yu, Lei Ke, Haolin Liu, Yujun Zhou, Zhenwen Liang, Haitao Mi, Pratap Tokekar,
and Dong Yu. Stable and efficient single-rollout rl for multimodal reasoning. *arXiv preprint
arXiv:2512.18215*, 2025b.
- Jing-Cheng Pang, Pengyuan Wang, Kaiyuan Li, Xiong-Hui Chen, Jiacheng Xu, Zongzhang Zhang,
and Yang Yu. Language model self-improvement by reinforcement learning contemplation. *arXiv
preprint arXiv:2305.14483*, 2023.
- Jaesung R Park, Junsu Kim, Gyeongman Kim, Jinyoung Jo, Sean Choi, Jaewoong Cho, and Ernest K
Ryu. Clip-low increases entropy and clip-high decreases entropy in reinforcement learning of
large language models. *arXiv preprint arXiv:2509.26114*, 2025.

- Mihir Prabhudesai, Lili Chen, Alex Ippoliti, Katerina Fragkiadaki, Hao Liu, and Deepak Pathak. Maximizing confidence alone improves reasoning. *arXiv preprint arXiv:2505.22660*, 2025.
- Justin K Pugh, Lisa B Soros, and Kenneth O Stanley. Quality diversity: A new frontier for evolutionary computation. *Frontiers in Robotics and AI*, 3:40, 2016.
- David Rein, Betty Li Hou, Asa Cooper Stickland, Jackson Petty, Richard Yuanzhe Pang, Julien Dirani, Julian Michael, and Samuel R Bowman. Gpqa: A graduate-level google-proof q&a benchmark. In *First Conference on Language Modeling*, 2024.
- Sheikh Shafayat, Fahim Tajwar, Ruslan Salakhutdinov, Jeff Schneider, and Andrea Zanette. Can large reasoning models self-train? *arXiv preprint arXiv:2505.21444*, 2025.
- Zhihong Shao, Peiyi Wang, Qihao Zhu, Runxin Xu, Junxiao Song, Xiao Bi, Haowei Zhang, Mingchuan Zhang, YK Li, Yang Wu, et al. Deepseekmath: Pushing the limits of mathematical reasoning in open language models. *arXiv preprint arXiv:2402.03300*, 2024.
- Ilya Shumailov, Zakhar Shumaylov, Yiren Zhao, Nicolas Papernot, Ross Anderson, and Yarin Gal. Ai models collapse when trained on recursively generated data. *Nature*, 631(8022):755–759, 2024.
- P Team, Xinrun Du, Yifan Yao, Kaijing Ma, Bingli Wang, Tianyu Zheng, King Zhu, Minghao Liu, Yiming Liang, Xiaolong Jin, Zhenlin Wei, Chujie Zheng, Kaixin Deng, Shawn Gavin, Shian Jia, Sichao Jiang, Yiyan Liao, Rui Li, Qinrui Li, Sirun Li, Yizhi Li, Yunwen Li, David Ma, Yuansheng Ni, Haoran Que, Qiyao Wang, Zhoufutu Wen, Siwei Wu, Tyshawn Hsing, Ming Xu, Zhenzhu Yang, Zekun Moore Wang, Juntong Zhou, Yuelin Bai, Xingyuan Bu, Chenglin Cai, Liang Chen, Yifan Chen, Chengtuo Cheng, Tianhao Cheng, Keyi Ding, Siming Huang, Yun Huang, Yaoru Li, Yizhe Li, Zhaoqun Li, Tianhao Liang, Chengdong Lin, Hongquan Lin, Yinghao Ma, Tianyang Pang, Zhongyuan Peng, Zifan Peng, Qige Qi, Shi Qiu, Xingwei Qu, Shanghaoran Quan, Yizhou Tan, Zili Wang, Chenqing Wang, Hao Wang, Yiya Wang, Yubo Wang, Jiajun Xu, Kexin Yang, Ruibin Yuan, Yuanhao Yue, Tianyang Zhan, Chun Zhang, Jinyang Zhang, Xiyue Zhang, Xingjian Zhang, Yue Zhang, Yongchi Zhao, Xiangyu Zheng, Chenghua Zhong, Yang Gao, Zhoujun Li, Dayiheng Liu, Qian Liu, Tianyu Liu, Shiwen Ni, Junran Peng, Yujia Qin, Wenbo Su, Guoyin Wang, Shi Wang, Jian Yang, Min Yang, Meng Cao, Xiang Yue, Zhaoxiang Zhang, Wangchunshu Zhou, Jiaheng Liu, Qunshu Lin, Wenhao Huang, and Ge Zhang. Supergpqa: Scaling llm evaluation across 285 graduate disciplines, 2025. URL <https://arxiv.org/abs/2502.14739>.
- Shenzhi Wang, Le Yu, Chang Gao, Chujie Zheng, Shixuan Liu, Rui Lu, Kai Dang, Xionghui Chen, Jianxin Yang, Zhenru Zhang, et al. Beyond the 80/20 rule: High-entropy minority tokens drive effective reinforcement learning for llm reasoning. *arXiv preprint arXiv:2506.01939*, 2025a.
- Xiangqi Wang, Yue Huang, Yanbo Wang, Xiaonan Luo, Kehan Guo, Yujun Zhou, and Xiangliang Zhang. Adareasoner: Adaptive reasoning enables more flexible thinking. *arXiv preprint arXiv:2505.17312*, 2025b.
- Xiangqi Wang, Yue Huang, Yujun Zhou, Xiaonan Luo, Kehan Guo, and Xiangliang Zhang. Causally-enhanced reinforcement policy optimization. *arXiv preprint arXiv:2509.23095*, 2025c.
- Yizhong Wang, Yeganeh Kordi, Swaroop Mishra, Alisa Liu, Noah A Smith, Daniel Khashabi, and Hannaneh Hajishirzi. Self-instruct: Aligning language models with self-generated instructions. In *Proceedings of the 61st annual meeting of the association for computational linguistics (volume 1: long papers)*, pp. 13484–13508, 2023.
- Yubo Wang, Xueguang Ma, Ge Zhang, Yuansheng Ni, Abhranil Chandra, Shiguang Guo, Weiming Ren, Aaran Arulraj, Xuan He, Ziyang Jiang, Tianle Li, Max Ku, Kai Wang, Alex Zhuang, Rongqi Fan, Xiang Yue, and Wenhui Chen. MMLU-pro: A more robust and challenging multi-task language understanding benchmark. In *The Thirty-eight Conference on Neural Information Processing Systems Datasets and Benchmarks Track*, 2024. URL <https://openreview.net/forum?id=y10DM6R2r3>.

- Zengzhi Wang, Fan Zhou, Xuefeng Li, and Pengfei Liu. Octothinker: Mid-training incentivizes reinforcement learning scaling. *arXiv preprint arXiv:2506.20512*, 2025d.
- Guangzhi Xiong, Qiao Jin, Xiao Wang, Yin Fang, Haolin Liu, Yifan Yang, Fangyuan Chen, Zhixing Song, Dengyu Wang, Minjia Zhang, et al. Rag-gym: Optimizing reasoning and search agents with process supervision. *arXiv preprint arXiv:2502.13957*, 2025.
- An Yang, Anfeng Li, Baosong Yang, Beichen Zhang, Binyuan Hui, Bo Zheng, Bowen Yu, Chang Gao, Chengen Huang, Chenxu Lv, et al. Qwen3 technical report. *arXiv preprint arXiv:2505.09388*, 2025.
- Qiyang Yu, Zheng Zhang, Ruofei Zhu, Yufeng Yuan, Xiaochen Zuo, Yu Yue, Weinan Dai, Tiantian Fan, Gaohong Liu, Lingjun Liu, et al. Dapo: An open-source llm reinforcement learning system at scale. *arXiv preprint arXiv:2503.14476*, 2025.
- Weihao Zeng, Yuzhen Huang, Qian Liu, Wei Liu, Keqing He, Zejun Ma, and Junxian He. Simplerl-zoo: Investigating and taming zero reinforcement learning for open base models in the wild. *arXiv preprint arXiv:2503.18892*, 2025.
- Kongcheng Zhang, Qi Yao, Shunyu Liu, Yingjie Wang, Baisheng Lai, Jieping Ye, Mingli Song, and Dacheng Tao. Consistent paths lead to truth: Self-rewarding reinforcement learning for llm reasoning. *arXiv preprint arXiv:2506.08745*, 2025a.
- Qingyang Zhang, Haitao Wu, Changqing Zhang, Peilin Zhao, and Yatao Bian. Right question is already half the answer: Fully unsupervised llm reasoning incentivization. *arXiv preprint arXiv:2504.05812*, 2025b.
- Wenting Zhao, Pranjal Aggarwal, Swarnadeep Saha, Asli Celikyilmaz, Jason Weston, and Ilia Kulikov. The majority is not always right: RL training for solution aggregation. *arXiv preprint arXiv:2509.06870*, 2025a.
- Xuandong Zhao, Zhewei Kang, Aosong Feng, Sergey Levine, and Dawn Song. Learning to reason without external rewards. *arXiv preprint arXiv:2505.19590*, 2025b.
- Yulai Zhao, Haolin Liu, Dian Yu, SY Kung, Haitao Mi, and Dong Yu. One token to fool llm-as-a-judge. *arXiv preprint arXiv:2507.08794*, 2025c.
- Tong Zheng, Lichang Chen, Simeng Han, R Thomas McCoy, and Heng Huang. Learning to reason via mixture-of-thought for logical reasoning. *arXiv preprint arXiv:2505.15817*, 2025a.
- Tong Zheng, Hongming Zhang, Wenhao Yu, Xiaoyang Wang, Xinyu Yang, Runpeng Dai, Rui Liu, Huiwen Bao, Chengsong Huang, Heng Huang, et al. Parallel-r1: Towards parallel thinking via reinforcement learning. *arXiv preprint arXiv:2509.07980*, 2025b.
- Xiangxin Zhou, Zichen Liu, Anya Sims, Haonan Wang, Tianyu Pang, Chongxuan Li, Liang Wang, Min Lin, and Chao Du. Reinforcing general reasoning without verifiers. *arXiv preprint arXiv:2505.21493*, 2025a.
- Yujun Zhou, Yufei Han, Haomin Zhuang, Kehan Guo, Zhenwen Liang, Hongyan Bao, and Xiangliang Zhang. Defending jailbreak prompts via in-context adversarial game. *arXiv preprint arXiv:2402.13148*, 2024.
- Yujun Zhou, Jiayi Ye, Zipeng Ling, Yufei Han, Yue Huang, Haomin Zhuang, Zhenwen Liang, Kehan Guo, Taicheng Guo, Xiangqi Wang, et al. Dissecting logical reasoning in llms: A fine-grained evaluation and supervision study. *arXiv preprint arXiv:2506.04810*, 2025b.
- Haomin Zhuang, Yujun Zhou, Taicheng Guo, Yue Huang, Fangxu Liu, Kai Song, and Xiangliang Zhang. Exploring multi-temperature strategies for token-and rollout-level control in rlvr. *arXiv preprint arXiv:2510.08892*, 2025.

Yuxin Zuo, Kaiyan Zhang, Li Sheng, Shang Qu, Ganqu Cui, Xuekai Zhu, Haozhan Li, Yuchen Zhang, Xinwei Long, Ermo Hua, et al. Ttrl: Test-time reinforcement learning. *arXiv preprint arXiv:2504.16084*, 2025.

A Implementation Details

This section provides additional details on the implementation of our reward formulation and supporting mechanisms.

A.1 Training Configuration.

We conduct our experiments on two recent open-source base models: **Qwen3-4B-Base** and **Qwen3-8B-Base**. Our training process is implemented using the GRPO algorithm. We adopt a setup similar to that of TTRL for generating training signals. For each problem instance, we first perform a roll-out phase where the policy generates 64 candidate responses. A majority label is then determined by performing a majority vote on the final answers extracted from these 64 samples. Subsequently, a random subset of 32 of these responses is used to form a batch for a single model update step. To ensure that the model has sufficient capacity for complex, multi-step reasoning, we set the maximum response length to 12,288 tokens during generation. To guide the model’s reasoning process, we utilize the system prompt from SimpleRL-Zoo (Zeng et al., 2025). Implementation details are discussed in Appendix A.

A.2 System Prompt

For all experiments, we used the following system prompt to guide the model’s generation format, ensuring that it produces a step-by-step reasoning process and a clearly marked final answer (Zeng et al., 2025):

System Prompt

Please reason step by step, and put your final answer within `\boxed{}`.

A.3 Answer and Reasoning Extraction

To implement the scoring criteria described in the main text, we apply the following extraction procedure for each generated response o_i :

- **Final Answer Extraction (for Validity):** We parse the response to find the content within the final occurrence of the `\boxed{.}` command. A response is deemed "valid" only if this command is present and its content contains at least one numeric digit. This extracted numeric string is used for the majority vote.

A.4 Novelty Score Calculation Details

The novelty score u_i relies on computing semantic similarity between the reasoning parts of the generated responses.

Embedding Model. We use the **Qwen3-4B-Embedding** model to generate dense vector representations for the extracted reasoning parts. Each vector is L2-normalized before similarity computation.

Cosine Similarity Matrix. For a group of G responses with corresponding L2-normalized embedding vectors $\{\mathbf{v}_1, \dots, \mathbf{v}_G\}$, the cosine similarity matrix $\mathbf{S} \in \mathbb{R}^{G \times G}$ is computed as $\mathbf{S} = \mathbf{V}\mathbf{V}^T$, where \mathbf{V} is the matrix whose rows are the vectors \mathbf{v}_i . The element S_{ij} represents the cosine similarity between the reasoning of response o_i and o_j .

Intra-Group Min-Max Normalization. To obtain the normalized novelty score $\tilde{u}_i \in [0, 1]$ from the raw scores $\{u_k\}$ within a specific group (e.g., the majority group), we apply standard min-max normalization:

$$\tilde{u}_i = \frac{u_i - \min(\{u_k\})}{\max(\{u_k\}) - \min(\{u_k\}) + \epsilon_{\text{norm}}}$$

where ϵ_{norm} is a small constant (e.g., 10^{-8}) to prevent division by zero in cases where all novelty scores in the group are identical.

A.5 Hyperparameter Settings

For our label-free experiments, we largely follow the settings established by TTRL to ensure a fair comparison. The general hyperparameters are detailed in Table 4, and the settings specific to our EVOL-RL method are listed in Table 5.

Table 4: General hyperparameters for label-free training, following TTRL.

Hyperparameter	Value
Train Batch Size	8
PPO Mini-Batch Size	1 (effective size of 32)
PPO Micro-Batch Size	2
Rollouts for Majority Vote	64
Rollouts Used for Training	32
Generation Temperature	1.0
Validation Temperature	0.6
Learning Rate	5e-7
Use KL Loss	True
KL Loss Coefficient	0.001

Table 5: Key hyperparameters specific to the EVOL-RL framework.

Hyperparameter	Value
Asymmetric Clipping High (ϵ_{high})	0.28
Entropy Regularizer Coefficient (λ_{ent})	0.003
Novelty Score Mixing Coefficient (α)	0.5

A.6 Computational Resources

All experiments reported in this paper were conducted on a single server equipped with 8x NVIDIA H20 GPUs.

B Additional Experimental Results

B.1 Effectiveness on Different Model Architectures

To verify that our approach is not limited to a single model family, we conducted an additional experiment applying EVOL-RL and TTRL to the **OctoThinker-8B-Hybrid-Base** model (Wang et al., 2025d), a different architecture from the Qwen3 series. We used the same label-free training setup on the MATH-500 dataset.

The results, presented in Table 6, strongly confirm our core thesis. The TTRL baseline, when applied to OctoThinker, exhibits the classic symptoms of entropy collapse: while it significantly improves

Table 6: Comparison of models trained with TTRL and EVOL-RL on MATH-500 on OctoThinker-8B-Hybrid-Base. Each cell shows pass@1/pass@16 (averaged over 32 rollouts). Δ uses red (+) for positive and blue for negative values.

Model	MATH	AIME24	AIME25	AMC	GPQA
OctoThinker-8B-Hybrid-Base					
Base Model	33.8/79.8	1.5/13.5	1.3/13.9	16.2/56.9	26.3/85.7
w/TTRL	63.8/76.4	2.8/10.8	2.1/11.0	27.9/54.7	31.9/71.5
w/EVOL-RL	63.2/86.3	9.0/30.3	7.2/22.4	34.1/65.6	33.2/85.7
Δ	-0.6/+9.9	+6.2/+19.5	+5.1/+11.4	+6.2/+10.9	+1.3/+14.2

Table 7: Extended comparison of baseline methods on Qwen3-4B-Base, trained in a label-free setting using MATH-Train. Each cell shows pass@1/pass@16, and the highest value in each column is bolded.

Model	MATH	AIME24	AIME25	AMC	GPQA
Qwen3-4B-Base					
Base Model	67.4/89.6	10.0/32.4	5.5/30.0	39.3/75.2	34.4/85.6
w/TTRL	75.4/86.9	12.1/23.2	6.8/28.6	42.5/75.2	36.5/81.4
w/EM-RL-Token	76.0/90.6	12.5/31.3	10.5/30.8	46.6/77.7	36.8/82.6
w/EM-RL-Sequence	67.4/89.9	10.6/31.4	7.1/28.8	39.6/73.7	34.5/86.2
w/Self-Consistency	76.0/89.7	12.5/30.4	10.4/33.6	48.1/78.1	35.9/81.2
w/EVOL-RL	80.0/93.3	20.7/47.6	17.5/39.9	51.4/80.3	37.2/88.7

in-domain pass@1 accuracy (e.g., on MATH, from 33.8% to 63.8%), it fails to improve multi-path accuracy. In fact, pass@16 performance degrades on AIME24 (from 13.5% to 10.8%) and GPQA (from 85.7% to 71.5%) compared to the base model.

In sharp contrast, EVOL-RL successfully prevents this collapse and translates exploration into robust performance gains. While achieving a comparable pass@1 improvement on MATH, EVOL-RL yields massive improvements in pass@16 across all benchmarks. Most notably, it achieves a +19.5% gain on AIME24 and a +11.4% gain on AIME25 in pass@16 accuracy over TTRL.

This experiment demonstrates that entropy collapse is a fundamental flaw of the majority-only objective and that EVOL-RL is a robust and generalizable solution that functions effectively across different model architectures.

B.2 Comparison with Other Self-Improvement Baselines

To demonstrate that EVOL-RL is not just an improvement over TTRL but a more robust solution to the "entropy collapse" problem, we compare it against a broader suite of label-free self-improvement methods. These include methods based on self-consistency (Self-Consistency (Wang et al., 2023; Huang et al., 2023)) and intrinsic confidence (EM-RL-Token and EM-RL-Sequence (Agarwal et al., 2025)). We trained all methods on the Qwen3-4B-Base model under the same label-free setting, with results presented in Table 7.

The results highlight a clear and consistent pattern: methods that optimize for a single signal (like consensus or confidence) fail to achieve robust, generalizable gains.

While baselines like TTRL, EM-RL-Token, and Self-Consistency all show moderate improvements in pass@1 accuracy on some benchmarks, they don't show any consistent improvement in pass@16 performance, which is an indicator of entropy collapse. On the challenging AIME24 benchmark, every single one of these baselines performs worse than the original Base Model on pass@16 (e.g.,

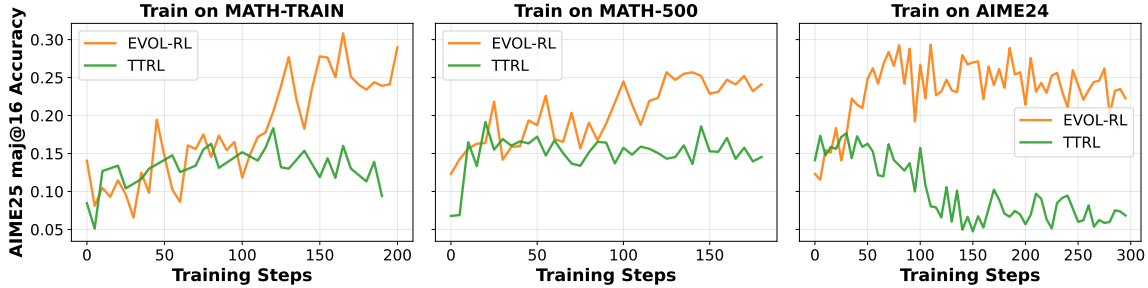


Figure 5: Training dynamics of the majority-vote accuracy (maj@16) for EVOL-RL and TTRL. Each panel plots the accuracy of the consensus answer derived from 16 rollouts over the course of training. The training datasets are: (Left) MATH-TRAIN, (Middle) MATH-500, and (Right) AIME24.

23.2% for TTRL and 30.4% for Self-Consistency, vs. 32.4% for the Base Model). This strongly suggests that their singular focus on "certainty" actively degrades solution diversity and multi-path reasoning.

In stark contrast, EVOL-RL is the only method that robustly improves both single-shot accuracy (pass@1) and multi-path reliability (pass@16) across all benchmarks. The gains are most pronounced on out-of-domain tasks. On AIME24, EVOL-RL achieves a pass@1 of **20.7%** (vs. $\sim 12.5\%$ for the next-best baselines) and a pass@16 of **47.6%**, demonstrating a massive +15% improvement over even the Base Model, whereas all other methods failed. This result strongly supports our central thesis: a simple consensus or confidence signal is insufficient. True self-improvement requires an explicit mechanism—like our *majority-for-stability* + *novelty-for-exploration* rule—to prevent entropy collapse and foster diverse, generalizable reasoning.

B.3 Analysis of the Majority Vote Signal

To further investigate the differences between EVOL-RL and TTRL, we analyze the quality of the training signal itself by tracking the accuracy of the majority vote (maj@16) over the course of training, as shown in Figure 5. This analysis reveals how the self-generated pseudo-labels evolve under each method.

A highly consistent pattern emerges across all three training datasets. TTRL initially improves the maj@16 accuracy over the base model, but it quickly converges to a performance plateau. For the remainder of the training, its maj@16 accuracy remains largely unchanged, indicating that the consensus-only approach rapidly finds a local optimum for the consensus answer and becomes locked in, unable to discover better solutions.

In contrast, EVOL-RL exhibits a markedly different dynamic. While its initial trajectory often mirrors that of TTRL, reflecting the early stabilizing influence of the consensus signal, a clear divergence occurs. Consistent with the inflection point observed in our main training dynamics analysis, EVOL-RL’s maj@16 accuracy breaks away from the TTRL plateau and begins a second, sustained ascent. It reliably climbs to and stabilizes at a significantly higher level of accuracy. This demonstrates that EVOL-RL’s exploration mechanisms not only improve the final policy but also progressively refine the quality of the pseudo-labels used for training, allowing the model to escape suboptimal consensus and continuously improve its understanding of the task.

B.4 Training Dynamics of 8B Models

The training dynamics of the 8B models, presented in Figure 6, largely mirror the patterns observed with the 4B models, confirming that the core mechanisms of EVOL-RL are robust to scale.

Across all three training datasets (MATH-TRAIN, MATH-500, and AIME24), we observe the same two-stage process. In Stage 1, both TTRL and EVOL-RL experience an initial drop in policy entropy

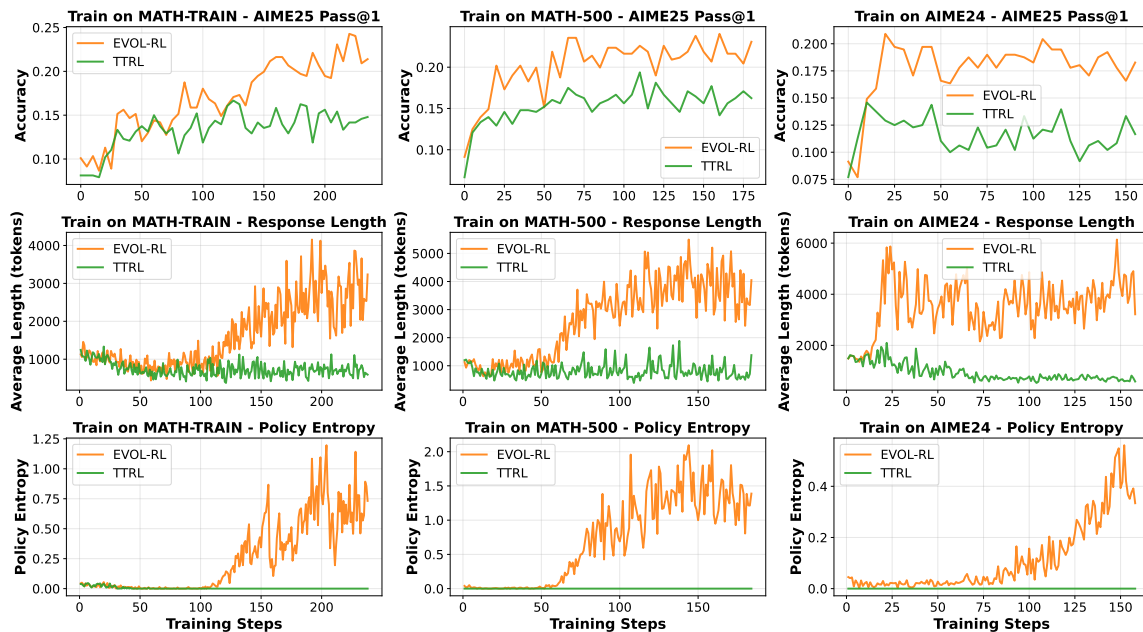


Figure 6: Training dynamics for EVOL-RL and TTRL on Qwen3-8B-Base model. **Left:** models trained on *MATH-TRAIN*. **Middle:** models trained on *MATH-500*. **Right:** models trained on *AIME24*. Each panel plots, over training steps, (i) Pass@1 on AIME25, (ii) average response length on the training set, and (iii) policy entropy on the training set.

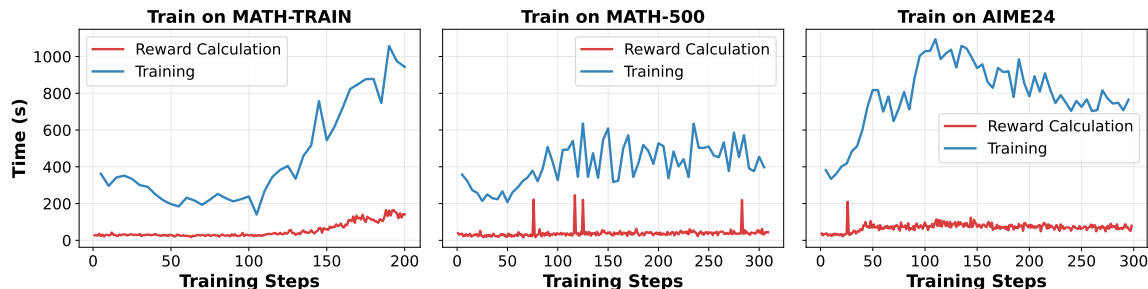


Figure 7: Wall-clock time (seconds) per training step for **Novelty Reward Calculation** (Red) versus the **Total Training Process** (Blue) across three datasets. While both costs naturally increase as the model evolves to generate longer reasoning paths, the reward calculation overhead remains a minor fraction of the total computational load.

and response length due to the strong initial pressure of the majority-vote signal. TTRL becomes permanently trapped in this low-entropy, low-complexity state.

In Stage 2, EVOL-RL consistently diverges at an "evolving point." Its policy entropy begins a sustained recovery, followed by a coordinated increase in average response length and out-of-domain accuracy on AIME25. This confirms that even at a larger scale, EVOL-RL successfully prevents entropy collapse and fosters a positive feedback loop where exploration, reasoning complexity, and performance reinforce one another, while the consensus-only TTRL approach stagnates.

B.5 Analysis of the Computational Overhead from the Novelty Reward

A practical consideration for our method is the additional computational load introduced by the embedding-based novelty reward. To rigorously quantify this, we tracked the wall-clock time per

training step, decomposing it into two parts: (1) the Novelty Reward Calculation (comprising $B \times N$ embedding model calls and the $O(BN^2)$ similarity matrix computation, where B is the batch size and N is the number of rollouts), and (2) the Total Training Process (including rollout generation, reward calculation and model updates). The results are plotted in Figure 7.

The analysis reveals two key insights:

- **Scaling with Reasoning Length:** As expected, both curves rise over time. This correlates with our findings in Figure 3 that the model learns to generate significantly longer CoT during training. Longer responses require more time to generate (Training) and more time to embed (Reward Calculation).
- **Low Relative Overhead:** while the reward cost scales with response length (requiring embedding of longer sequences), the Novelty Reward Calculation (red curve) remains a small portion of the overall runtime, stabilizing around 100 seconds.

The occasional sharp spikes in the Red curve are anomalous and likely attributable to external API connection instabilities. We conclude that the embedding-based reward introduces a manageable overhead that is marginal compared to the inherent cost of training reasoning models, especially given the substantial gains in performance and generalization it unlocks.

B.6 Case Study: Validity of the Semantic Novelty Proxy

A potential concern regarding our method is whether semantic similarity in an embedding space is a meaningful proxy for genuine reasoning novelty. To validate this, we conducted a case study, shown in Figure 8, by generating 8 rollouts for a single AIME25 problem using Qwen3-4B-Instruct-2407 and computing their reasoning path similarity matrix with Qwen3-4B-Embedding.

The results provide strong empirical evidence for the validity of this proxy. As shown in the figure, the matrix reveals distinct, high-similarity clusters that align with the reasoning logic. Specifically, the 6 rollouts that produced the same final answer ("19") have an extremely high intra-cluster similarity (the 6x6 block at the top-left). Crucially, these paths are semantically distinct from the path that answered "31" and the path that answered "7221", showing clear separation in the embedding space.

This demonstrates that the embedding space does successfully capture and cluster the core logic of the reasoning paths, distinguishing between different reasoning trajectories.

C Additional Rationale Supporting the Reward Design

C.1 Analysis of Reward Formulation on "Almost Correct" Solutions

A key nuance in our reward formulation is how it handles solutions that are "almost correct"—for instance, a minority solution that is semantically similar to a correct majority path but fails on a minor step. This section provides a detailed analysis of how our two-part novelty score, $u_i = 1 - (\alpha \bar{s}_i + (1 - \alpha)m_i)$, is specifically designed to handle this nuance.

Our primary goal is to apply strong negative pressure against high-frequency, common failure modes, not to indiscriminately punish all incorrect explorations. In the scenario where a minority solution is semantically similar to the majority (resulting in a high global similarity m_i), the intra-group mean similarity \bar{s}_i (the solution's average similarity to other minority solutions) becomes the critical differentiator. We analyze two distinct cases:

- **Case 1: The error is a rare, exploratory mistake.** If the "almost correct" error is a rare, occasional mistake, the reasoning path will be semantically dissimilar from the other failure modes in the minority group. This results in a low \bar{s}_i . According to our novelty formula, this low \bar{s}_i counteracts the high m_i , leading to a higher overall novelty score u_i . This ef-

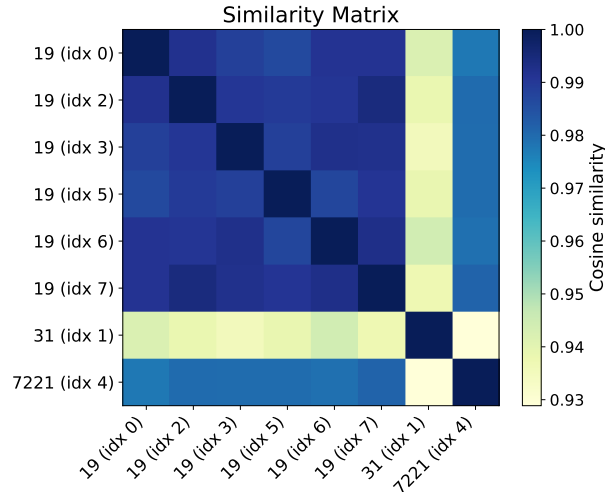


Figure 8: Case study of the reasoning path cosine similarity matrix for 8 rollouts on a single AIME25 problem. The axes are labeled with the `final_answer(index_i)` for each rollout. The 8 rollouts produced three distinct final answers: "19" (6 times), "31" (1 time), and "7221" (1 time).

fectively mitigates the penalty, ensuring the model is not strongly discouraged from valid exploration.

- **Case 2: The error is a common failure mode.** If the error represents a high-frequency failure mode (e.g., a consistent arithmetic error), the reasoning path will be semantically similar to many other solutions in the minority group. This results in a high \bar{s}_i . In this case, both the \bar{s}_i and m_i terms are high, leading to a very low u_i . This results in a maximum penalty, preventing the model from collapsing into a "consistent but wrong" state.

This design ensures that our reward mechanism is robust. It relies on the group-level context to selectively protect valuable explorations while aggressively pruning systematic errors. This is particularly crucial in high-uncertainty scenarios where the novelty signal must accurately guide exploration, which is the exact behavior we aim to encourage.

D Theoretical Justification

In this section, we formally justify the different behaviors of the optimal policy under correctness-only reinforcement learning and under our similarity-augmented objective. We show that, for a suitably small similarity weight and under a simple similarity-gap structure, both objectives have globally optimal policies that concentrate on the set of correct reasoning traces, but our similarity-augmented objective further selects solutions with strictly more diverse coverage over correct trajectories and, under additional symmetry condition, maximal policy entropy on the correct set.

D.1 Setup

For a given reasoning question q , there is a finite set \mathcal{Y} of complete chain-of-thought (CoT) trajectories for q . Each trajectory receives a binary task reward

$$r(y) \in \{0, 1\}, \quad y \in \mathcal{Y}.$$

We denote the correct set (answer-correct set) by

$$G := \{y \in \mathcal{Y} : r(y) = 1\},$$

and assume $G \neq \emptyset$. A policy π maps question to chain of thought reasoning. For simplicity, we will omit the condition of question in the following analysis.

Objectives. The correctness-only objective is

$$J_0(\pi) := \mathbb{E}_\pi[r(Y)] = \sum_{y \in \mathcal{Y}} \pi(y) r(y).$$

To encourage diverse correct solutions, we introduce a symmetric, nonnegative CoT-level dissimilarity

$$d : \mathcal{Y} \times \mathcal{Y} \rightarrow [0, \infty), \quad d(y, y') = d(y', y), \quad d(y, y) = 0,$$

and assume that d is bounded:

$$D_{\max} := \max_{y, y' \in \mathcal{Y}} d(y, y') < \infty. \quad (3)$$

Given a group size $K \geq 2$ and similarity weight $\lambda > 0$, we form i.i.d. samples $Y_1, \dots, Y_K \sim \pi$ and define the group reward

$$R_{\text{group}}(Y_{1:K}) := \frac{1}{K} \sum_{k=1}^K r(Y_k) + \lambda \cdot \frac{1}{K(K-1)} \sum_{k \neq \ell} d(Y_k, Y_\ell).$$

The correctness together with similarity objective is the expected group reward

$$J_\lambda(\pi) := \mathbb{E}_{Y_{1:K} \sim \pi}[R_{\text{group}}(Y_{1:K})].$$

The following standard computation shows that J_λ is a quadratic functional of π .

Lemma 1 (Expected group reward as a quadratic in π). *For any $\pi \in \Delta(\mathcal{Y})$,*

$$J_\lambda(\pi) = \sum_y \pi(y) r(y) + \lambda \sum_{y, y'} \pi(y) \pi(y') d(y, y'). \quad (4)$$

Proof. By linearity of expectation and the i.i.d. assumption on $Y_{1:K}$, the first term yields

$$\mathbb{E} \left[\frac{1}{K} \sum_{k=1}^K r(Y_k) \right] = \mathbb{E}[r(Y_1)] = \sum_y \pi(y) r(y).$$

For the second term, each ordered pair (k, ℓ) with $k \neq \ell$ has the same distribution, so

$$\mathbb{E} \left[\frac{1}{K(K-1)} \sum_{k \neq \ell} d(Y_k, Y_\ell) \right] = \mathbb{E}[d(Y_1, Y_2)] = \sum_{y, y'} \pi(y) \pi(y') d(y, y'),$$

which gives (4). □

D.2 Step 1: Global maximizers concentrate on the correct set

We first show that for a suitable range of λ , any global maximizer of J_0 or J_λ puts zero probability on incorrect trajectories.

Lemma 2 (Global maximizers of J_0 are supported on G). *Assume $G \neq \emptyset$. Then any global maximizer π^* of J_0 satisfies*

$$\text{supp}(\pi^*) \subseteq G.$$

Moreover, the set of global maximizers of J_0 is exactly $\Delta(G)$.

Proof. For any $\pi \in \Delta(\mathcal{Y})$,

$$J_0(\pi) = \sum_y \pi(y) r(y) = \sum_{y \in G} \pi(y) = \pi(G) \leq 1,$$

with equality iff $\pi(G) = 1$, i.e., $\text{supp}(\pi) \subseteq G$. Because $G \neq \emptyset$, there exists a policy with $\pi(G) = 1$ and $J_0(\pi) = 1$, so the maximal value of J_0 is 1, achieved exactly by policies supported on G . □

For the similarity-augmented objective, the task reward gap between correct and incorrect trajectories is 1, while the similarity term is bounded by D_{\max} from (3). For sufficiently small λ , the former always dominates the latter.

Lemma 3 (For small λ , global maximizers of J_λ are supported on G). *Suppose $G \neq \emptyset$ and D_{\max} is defined as in (3). If*

$$0 < \lambda < \frac{1}{2D_{\max}}, \quad (5)$$

(with the convention that the condition is vacuous if $D_{\max} = 0$), then any global maximizer π^* of J_λ satisfies

$$\text{supp}(\pi^*) \subseteq G.$$

Proof. Using (4), we can write

$$J_\lambda(\pi) = \sum_y \pi(y)r(y) + \lambda \sum_{y,y'} \pi(y)\pi(y')d(y,y').$$

For $y \in \mathcal{Y}$, the partial derivative of J_λ w.r.t. $\pi(y)$ is

$$g_y(\pi) := \frac{\partial J_\lambda(\pi)}{\partial \pi(y)} = r(y) + 2\lambda \sum_{y'} \pi(y')d(y,y'),$$

where we used the symmetry $d(y,y') = d(y',y)$.

Assume for contradiction that π^* is a global maximizer of J_λ and there exists an incorrect trajectory $y_0 \notin G$ with $\pi^*(y_0) > 0$. Because $G \neq \emptyset$, pick any $y_1 \in G$ (so $r(y_1) = 1$). Consider the feasible direction in the simplex

$$v := e_{y_1} - e_{y_0},$$

which corresponds to infinitesimally moving probability mass from y_0 to y_1 . For sufficiently small $\varepsilon > 0$, the perturbed policy $\pi^* + \varepsilon v$ remains in $\Delta(\mathcal{Y})$.

The directional derivative of J_λ at π^* along v is

$$\left. \frac{d}{d\varepsilon} J_\lambda(\pi^* + \varepsilon v) \right|_{\varepsilon=0} = \langle \nabla J_\lambda(\pi^*), v \rangle = g_{y_1}(\pi^*) - g_{y_0}(\pi^*).$$

By definition of g_y ,

$$\begin{aligned} g_{y_1}(\pi^*) - g_{y_0}(\pi^*) &= (r(y_1) - r(y_0)) + 2\lambda \sum_{y'} \pi^*(y')(d(y_1,y') - d(y_0,y')) \\ &= 1 + 2\lambda \sum_{y'} \pi^*(y')(d(y_1,y') - d(y_0,y')), \end{aligned}$$

since $r(y_1) = 1$ and $r(y_0) = 0$. By the definition of D_{\max} ,

$$|d(y_1,y') - d(y_0,y')| \leq D_{\max} \quad \text{for all } y',$$

and since $\sum_{y'} \pi^*(y') = 1$, we obtain

$$\left| \sum_{y'} \pi^*(y')(d(y_1,y') - d(y_0,y')) \right| \leq D_{\max}.$$

Hence

$$g_{y_1}(\pi^*) - g_{y_0}(\pi^*) \geq 1 - 2\lambda D_{\max}.$$

If $0 < \lambda < 1/(2D_{\max})$, then $1 - 2\lambda D_{\max} > 0$, so

$$\langle \nabla J_\lambda(\pi^*), v \rangle > 0.$$

Thus moving a small amount of mass from y_0 to y_1 strictly increases J_λ , contradicting the assumption that π^* is a (global, hence local) maximizer. Therefore no maximizer can assign positive probability to any incorrect trajectory, and $\text{supp}(\pi^*) \subseteq G$. \square

Combining Lemma 2 and Lemma 3, we obtain that assume $G \neq \emptyset$, $D_{\max} < \infty$, and (5). Then any global maximizer of J_0 or J_λ is supported on G . Thus we may restrict attention to

$$\Delta(G) := \{\pi \in \Delta(\mathcal{Y}) : \text{supp}(\pi) \subseteq G\}$$

when comparing optimal policies.

D.3 Step 2: Mode structure inside G and a piecewise-homogeneous similarity gap

We now formalize the assumption that the correct set G contains multiple qualitatively distinct solution modes, with large similarity gaps between modes and relatively homogeneous dissimilarity within each mode.

Assumption 1 (Mode partition of correct CoTs). *The correct set G is partitioned into $M \geq 2$ disjoint subsets*

$$G = G_1 \cup \dots \cup G_M, \quad G_m \cap G_{m'} = \emptyset \ (m \neq m'),$$

where each G_m corresponds to a distinct reasoning mode (solution pattern). Let $N_m := |G_m|$ and $N := |G| = \sum_{m=1}^M N_m$.

For any $\pi \in \Delta(G)$, we define the total probability mass on each mode:

$$w_m(\pi) := \sum_{y \in G_m} \pi(y), \quad m = 1, \dots, M.$$

Then $w(\pi) = (w_1(\pi), \dots, w_M(\pi))$ lies in the simplex

$$\Delta_M := \{w \in \mathbb{R}_+^M : \sum_{m=1}^M w_m = 1\}.$$

We impose a piecewise-homogeneous similarity-gap assumption on d within G .

Assumption 2 (Piecewise-homogeneous dissimilarity on the correct set). *There exist constants $D_{\text{in}} \geq 0$ and $D_{\text{out}} > D_{\text{in}}$ such that for all $y, y' \in G$,*

$$d(y, y') = \begin{cases} 0, & \text{if } y = y', \\ D_{\text{in}}, & \text{if } y \neq y', y, y' \in G_m \text{ for some } m \text{ (same mode)}, \\ D_{\text{out}}, & \text{if } y \in G_m, y' \in G_{m'} \ (m \neq m') \text{ (different modes)}. \end{cases}$$

Assumption 2 idealizes the intuitive condition that trajectories within the same mode are relatively similar (with dissimilarity D_{in}), while trajectories from different modes are more dissimilar (with $D_{\text{out}} > D_{\text{in}}$).

Under these assumptions, the similarity term in J_λ over $\Delta(G)$ admits a convenient decomposition into a mode-level and an intra-mode component.

Lemma 4 (Decomposition of the dissimilarity term on G). *Under Assumptions 1 and 2, for any $\pi \in \Delta(G)$,*

$$\sum_{y, y' \in G} \pi(y)\pi(y')d(y, y') = D_{\text{out}} + (D_{\text{in}} - D_{\text{out}}) \sum_{m=1}^M w_m(\pi)^2 - D_{\text{in}} \sum_{y \in G} \pi(y)^2.$$

Consequently, on $\Delta(G)$,

$$J_\lambda(\pi) = 1 + \lambda \left[D_{\text{out}} + (D_{\text{in}} - D_{\text{out}}) \sum_{m=1}^M w_m(\pi)^2 - D_{\text{in}} \sum_{y \in G} \pi(y)^2 \right]. \quad (6)$$

Proof. Because $\text{supp}(\pi) \subseteq G$, we have $r(y) = 1$ on G and $r(y) = 0$ otherwise, hence $\sum_y \pi(y)r(y) = \sum_{y \in G} \pi(y) = 1$, giving the first term in (6).

For the dissimilarity term, we decompose by modes:

$$\sum_{y,y' \in G} \pi(y)\pi(y')d(y,y') = \sum_{m=1}^M \sum_{y,y' \in G_m} \pi(y)\pi(y')d(y,y') + \sum_{m \neq m'} \sum_{y \in G_m, y' \in G_{m'}} \pi(y)\pi(y')d(y,y').$$

Within a fixed mode G_m , we have $d(y,y) = 0$ and $d(y,y') = D_{\text{in}}$ for $y \neq y'$, so

$$\begin{aligned} \sum_{y,y' \in G_m} \pi(y)\pi(y')d(y,y') &= D_{\text{in}} \sum_{\substack{y,y' \in G_m \\ y \neq y'}} \pi(y)\pi(y') \\ &= D_{\text{in}} \left[\left(\sum_{y \in G_m} \pi(y) \right)^2 - \sum_{y \in G_m} \pi(y)^2 \right] \\ &= D_{\text{in}} \left[w_m(\pi)^2 - \sum_{y \in G_m} \pi(y)^2 \right]. \end{aligned}$$

Summing over m yields

$$\sum_{m=1}^M \sum_{y,y' \in G_m} \pi(y)\pi(y')d(y,y') = D_{\text{in}} \sum_{m=1}^M w_m(\pi)^2 - D_{\text{in}} \sum_{y \in G} \pi(y)^2.$$

Across different modes, $d(y,y') = D_{\text{out}}$ whenever $y \in G_m$ and $y' \in G_{m'}$ with $m \neq m'$, hence

$$\sum_{m \neq m'} \sum_{y \in G_m, y' \in G_{m'}} \pi(y)\pi(y')d(y,y') = D_{\text{out}} \sum_{m \neq m'} w_m(\pi)w_{m'}(\pi).$$

Since $\sum_m w_m(\pi) = 1$,

$$\sum_{m \neq m'} w_m w_{m'} = \left(\sum_m w_m \right)^2 - \sum_m w_m^2 = 1 - \sum_m w_m^2.$$

Combining the within-mode and cross-mode contributions gives

$$\begin{aligned} \sum_{y,y' \in G} \pi(y)\pi(y')d(y,y') &= D_{\text{in}} \sum_m w_m^2 - D_{\text{in}} \sum_{y \in G} \pi(y)^2 + D_{\text{out}} \left(1 - \sum_m w_m^2 \right) \\ &= D_{\text{out}} + (D_{\text{in}} - D_{\text{out}}) \sum_m w_m^2 - D_{\text{in}} \sum_{y \in G} \pi(y)^2. \end{aligned}$$

Substituting this into Lemma 1 with $\sum_y \pi(y)r(y) = 1$ yields (6). \square

Thus, over the feasible region $\Delta(G)$, maximizing $J_\lambda(\pi)$ is equivalent to maximizing

$$D_{\text{out}} + (D_{\text{in}} - D_{\text{out}}) \sum_{m=1}^M w_m(\pi)^2 - D_{\text{in}} \sum_{y \in G} \pi(y)^2,$$

or, equivalently (since $\lambda > 0$ and constants do not affect argmax), to minimizing

$$F(\pi) := (D_{\text{out}} - D_{\text{in}}) \sum_{m=1}^M w_m(\pi)^2 + D_{\text{in}} \sum_{y \in G} \pi(y)^2, \quad (7)$$

where $D_{\text{out}} - D_{\text{in}} > 0$ and $D_{\text{in}} \geq 0$.

D.4 Step 3: Coverage structure and entropy of optimal policies on G

Having reduced both objectives to $\Delta(G)$ (Lemma 2 and Lemma 3), we now compare their optimal solutions. First, Lemma 2 immediately implies:

Corollary 1 (Flat optimal set for correctness-only objective). *Under $G \neq \emptyset$, any $\pi \in \Delta(G)$ satisfies $J_0(\pi) = 1$ and is a global maximizer of J_0 . Hence J_0 is indifferent to how probability mass is distributed within G .*

In contrast, J_λ has a nontrivial preference both at the mode level and within each mode, captured by the quadratic form $F(\pi)$ in (7).

We first show that, for any fixed mode-mass vector w , J_λ is maximized by making the policy uniform within each mode.

Lemma 5 (Within each mode, optimal policies are uniform). *Fix $w \in \Delta_M$ and consider the set*

$$\mathcal{P}(w) := \{ \pi \in \Delta(G) : w_m(\pi) = w_m \text{ for all } m \}.$$

Under Assumptions 1 and 2, among all $\pi \in \mathcal{P}(w)$, $J_\lambda(\pi)$ is maximized (equivalently, $F(\pi)$ is minimized) by policies that are uniform within each mode:

$$\pi(y) = \frac{w_m}{N_m} \quad \text{for all } y \in G_m.$$

If $D_{\text{in}} > 0$, this choice is unique in $\mathcal{P}(w)$; if $D_{\text{in}} = 0$, J_λ is independent of the within-mode distribution.

Proof. For fixed w , the term $\sum_m w_m(\pi)^2$ in (7) is constant over $\mathcal{P}(w)$. Thus minimizing $F(\pi)$ over $\mathcal{P}(w)$ is equivalent to minimizing $\sum_{y \in G} \pi(y)^2$ over $\mathcal{P}(w)$.

Within each mode G_m , this is the classical problem of minimizing a sum of squares subject to a linear constraint:

$$\min \left\{ \sum_{y \in G_m} \pi(y)^2 : \sum_{y \in G_m} \pi(y) = w_m, \pi(y) \geq 0 \right\},$$

whose unique solution (when $w_m > 0$) is the uniform allocation $\pi(y) = w_m/N_m$ for all $y \in G_m$. If $D_{\text{in}} > 0$, this sum of squares enters $F(\pi)$ with a strictly positive coefficient, so any deviation from uniformity strictly increases $F(\pi)$. If $D_{\text{in}} = 0$, the intra-mode term vanishes from $F(\pi)$, and $F(\pi)$ (hence J_λ) depends only on w and not on the within-mode distribution. \square

By Lemma 5, any global maximizer of J_λ on $\Delta(G)$ must be uniform within each mode. We may therefore restrict attention to policies of the form

$$\pi(y) = \frac{w_m}{N_m} \quad \text{if } y \in G_m,$$

parameterized solely by $w \in \Delta_M$. Substituting this structure into (6) yields a purely mode-level objective.

Indeed, for such a π ,

$$\sum_{y \in G} \pi(y)^2 = \sum_{m=1}^M \sum_{y \in G_m} \left(\frac{w_m}{N_m} \right)^2 = \sum_{m=1}^M \frac{w_m^2}{N_m}.$$

Plugging this into Lemma 4 gives

$$\begin{aligned} J_\lambda(\pi) &= 1 + \lambda \left[D_{\text{out}} + (D_{\text{in}} - D_{\text{out}}) \sum_{m=1}^M w_m^2 - D_{\text{in}} \sum_{m=1}^M \frac{w_m^2}{N_m} \right] \\ &= 1 + \lambda \left[D_{\text{out}} - \sum_{m=1}^M a_m w_m^2 \right], \end{aligned} \tag{8}$$

where we define

$$a_m := (D_{\text{out}} - D_{\text{in}}) + \frac{D_{\text{in}}}{N_m} > 0.$$

Thus, among mode-wise uniform policies, maximizing J_λ is equivalent to minimizing

$$\sum_{m=1}^M a_m w_m^2 \quad \text{subject to } w \in \Delta_M.$$

Theorem 1 (Similarity reward selects high-coverage policies on G). *Suppose $G \neq \emptyset$, Assumptions 1 and 2 hold with $M \geq 2$, and λ satisfies (5). Let $\pi^{(\lambda)}$ be any global maximizer of J_λ over $\Delta(G)$, and let $w^{(\lambda)} := w(\pi^{(\lambda)})$ be its mode-mass vector. Then:*

1. $\pi^{(\lambda)}$ is uniform within each mode:

$$\pi^{(\lambda)}(y) = \frac{w_m^{(\lambda)}}{N_m} \quad \text{for all } y \in G_m, \quad m = 1, \dots, M.$$

2. $w^{(\lambda)}$ is the unique minimizer of $\sum_m a_m w_m^2$ over Δ_M :

$$w_m^{(\lambda)} = \frac{a_m^{-1}}{\sum_{j=1}^M a_j^{-1}}, \quad m = 1, \dots, M,$$

where $a_m > 0$ is defined above. In particular, every mode receives strictly positive probability:

$$w_m^{(\lambda)} > 0 \quad \text{for all } m = 1, \dots, M.$$

3. If, in addition, $D_{\text{in}} > 0$ and all modes have equal size $N_m \equiv N/M$, then all a_m coincide, $w^{(\lambda)}$ is uniform on modes, and $\pi^{(\lambda)}$ is the uniform distribution over all correct trajectories:

$$\pi^{(\lambda)}(y) = \frac{1}{|G|} \quad \text{for all } y \in G.$$

In this symmetric case, $\pi^{(\lambda)}$ maximizes the full policy entropy

$$H(\pi) := - \sum_{y \in G} \pi(y) \log \pi(y),$$

achieving $H(\pi^{(\lambda)}) = \log |G|$, the largest possible entropy on $\Delta(G)$.

In contrast, any $\pi^{(0)} \in \Delta(G)$ is optimal for J_0 , including degenerate solutions that concentrate on a single mode (with mode-level entropy 0 and very low trajectory-level entropy). Thus J_λ provably selects high-coverage policies within G , using all modes and being uniform within each mode, and, under mild symmetry, the maximum-entropy fully uniform policy, while J_0 does not enforce any coverage.

Proof. (i) By Lemma 3, any global maximizer $\pi^{(\lambda)}$ lies in $\Delta(G)$. Lemma 5 then implies that any maximizer must be uniform within each mode, so $\pi^{(\lambda)}$ has the stated form.

(ii) For such mode-wise uniform policies, (8) shows that maximizing J_λ is equivalent to minimizing $\sum_m a_m w_m^2$ over $w \in \Delta_M$. The function $w \mapsto \sum_m a_m w_m^2$ is strictly convex on Δ_M because each $a_m > 0$, and the constraint set Δ_M is convex and compact. Using Lagrange multipliers for the equality constraint $\sum_m w_m = 1$, the unique minimizer satisfies

$$2a_m w_m^{(\lambda)} + \mu = 0 \quad \text{for all } m,$$

for some scalar μ , which yields

$$w_m^{(\lambda)} = \frac{-\mu}{2a_m} = \frac{a_m^{-1}}{\sum_{j=1}^M a_j^{-1}}, \quad m = 1, \dots, M.$$

All $a_m > 0$, so all $w_m^{(\lambda)} > 0$.

(iii) If $D_{\text{in}} > 0$ and $N_m \equiv N/M$ for all m , then

$$a_m = (D_{\text{out}} - D_{\text{in}}) + \frac{D_{\text{in}}}{N_m} = (D_{\text{out}} - D_{\text{in}}) + \frac{D_{\text{in}}}{N/M}$$

is the same for all m . Hence $w_m^{(\lambda)} = 1/M$ for all m , and

$$\pi^{(\lambda)}(y) = \frac{w_m^{(\lambda)}}{N_m} = \frac{1/M}{N/M} = \frac{1}{N} = \frac{1}{|G|}$$

for all $y \in G$, i.e., $\pi^{(\lambda)}$ is the uniform distribution over G .

Finally, the Shannon entropy $H(\pi)$ over G is maximized on $\Delta(G)$ exactly by the uniform distribution, with value $\log |G|$. Thus $H(\pi^{(\lambda)}) = \log |G|$, the largest possible entropy on $\Delta(G)$. \square

Summary. Under the binary-reward setting and a piecewise-homogeneous similarity-gap structure on the correct set, we have shown that for any sufficiently small similarity weight λ :

- (a) (Lemma 2 and Lemma 3) Any global maximizer of J_0 or J_λ places all its probability mass on the correct set G ; i.e., both objectives “converge to the answer-correct set” in a static sense.
- (b) (Lemma 1) The correctness-only objective J_0 is completely flat on $\Delta(G)$: every distribution over G is globally optimal, including degenerate policies that collapse onto a single mode and assign zero probability to many correct trajectories.
- (c) (Theorem 1) In contrast, the similarity-augmented objective J_λ has global maximizers that must put positive mass on *all* modes and are uniform within each mode, and in the symmetric case where all modes have equal size, it selects the uniform distribution over all correct trajectories, which maximizes the full policy entropy.

Consequently, if a training procedure converges to global maximizers of J_0 and J_λ , then in the binary setting with similarity gaps: both trainings converge to fully correct policies, but the similarity-augmented training *provably selects* strictly more dispersed solutions on the correct set G , using all modes and, under mild symmetry, the maximum-entropy policy—while correctness-only training does not favor coverage and may converge to highly collapsed solutions.

E Use of Large Language Models in Preparation

We acknowledge the use of Large Language Models (LLMs) as assistants in the preparation of this manuscript. Their role included refining phrasing and improving the clarity of the text, as well as assisting with programming tasks such as code generation and debugging for our experiments. The authors critically reviewed, edited, and verified all LLM-generated content for accuracy and appropriateness, and take full responsibility for the final content of this paper.